RPP-RPT-34697, Rev. 0

Electrochemical Corrosion Report for Tanks 241-AW-103, 241-AZ-102, 241-AN-106, 241-AN-107, 241-AY-101, and 241-AY-102

J. B. Duncan
CH2M HILL Hanford Group, Inc.
Richland, WA 99352
U.S. Department of Energy Contract DE-AC27-99RL14047

|			
EDT/ECN:	DRF	UC:	
Cost Center:	7S110	Charge Code:	
B&R Code:		Total Pages:	3 7

Key Words: electrochemical, corrosion, supernatant, samples, liquid, saltcake, sludge, Tafel, layer, tanks, 241-AN-106, 241-AN-107, 241-AY-101, 241-AY-102, 241-AW-103, 241-AZ-102, carbon steel, settled solids, extrusion, testing, scans, hot cell, test coupons, ASTM G5-94, Stern-Geary calculations, electrochemistry

Abstract: Corrosion rates using supernatant samples retrieved from near the top of the liquid layer were determined for the tanks. Corrosion rates using settled solids (saltcake) were determined. The supernatant samples were tested as received without argon sparging. The settled solid sample segments were extruded under anaerobic condition and kept under a sweep of humidified argon gas during the electrochemical corrosion testing. The class of steel used to construct the tank in question was used, and test coupons were allowed to equilibrate for a minimum of 18 hours before a Tafel scan was initiated. The coupons were scanned from -250 mV to +250 mV from the rest or open circuit potential. The corrosion rate is reported along with the corrosion current measurement, open circuit potential, and a chi-square statistic generated by the instrument controlling and analysis algorithm.

AUG 2 2 2007

DATE:

STA: 15

HANFORD RELEASE

ID: 65
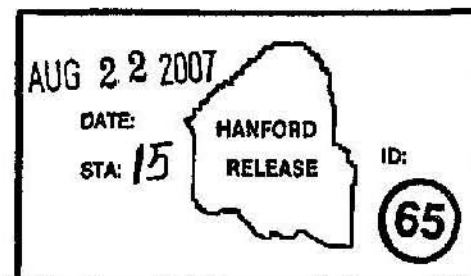
Release Approval   08/22/07   Date   Release Stamp

Approved For Public Release

RPP-RPT-34697
Revision 0

Electrochemical Corrosion Report for Tanks 241-AW-103, 241-AZ-102, 241-AN-106, 241-AN-107, 241-AY-101, and 241-AY-102

J. B. Duncan
CH2M HILL Hanford Group, Inc.

R. B. Wyrwas
RJ Lee Group, Inc.

CH2MHILL
Hanford Group, Inc.

RPP-PLAN-34697, Rev. 0

Table of Contents

List of Figures

List of Tables

RPP-RPT-34697, Rev. 0

List of Terms

Abbreviations

DST	double-shell tank
AN-106	241-AN-106
AN-107	241-AN-107
AW-103	241-AW-103
AY-101	241-AY-101
AY-102	241-AY-102
AZ-102	241-AZ-102
HHF	hydrostatic-head fluid
OCP	open circuit potential
SCE	saturated calomel electrode
WTP	Waste Treatment and Immobilization Plant

Units

mA	milliampere
mL	milliliter
mpy	mils per year
mV	millivolt
µA	microampere
V	volt

RPP-RPT-34697, Rev. 0

EXECUTIVE SUMMARY

Corrosion rates using supernatant samples retrieved from near the top of the liquid layer were determined by electrochemical methods for double-shell tanks 241-AN-106, 241-AN-107, 241-AY-101, 241-AY-102, 241-AW-103, and 241-AZ-102. Corrosion rates using settled solids (saltcake or sludge) were determined for tanks 241-AN-107, 241-AY-101, 241-AY-102, 241-AW-103, and 241-AZ-102. The electrochemical derived corrosion rates for tanks 241-AZ-102 and 241-AY-102 sludges were documented and are reported in RPP-20910, *Electrochemical Corrosion Studies, Core 313 Segments 19/19R1 and 19R3, Tank 241-AZ-102,* and RPP-18399, *Electrochemical Corrosion Studies, Core 308, Segments 14R1 and 14R2, Tank 241-AY-102,* respectively.

The supernatant samples were tested as received under quiescent conditions, i.e., without argon sparging. The settled solid sample segments were extruded under anaerobic condition where practicable and kept under a sweep of humidified argon gas during the electrochemical corrosion testing. The class of steel used to construct the tank in question was used, and test coupons were allowed to equilibrate for a minimum of 18 hours before a Tafel scan was initiated. The Tafel scan is takes into account the cathodic and anodic reactions over a pre-set potential range versus the rest potential (or open circuit potential).

The coupons were scanned from -250 mV to +250 mV from the rest or open circuit potential. The corrosion rate in mils per year is reported along with the corrosion current measurement, open circuit potential, and a chi-square statistic (a measure of the goodness of the result) generated by the instrument control and analysis algorithm.

The corrosion rate for supernatant samples ranged from 1.39E-01 mils per year (tank 241-AY-101) to 3.37E-03 mils per year (tank 241-AZ-102). The corrosion rate for the solids segment samples ranged from 1.1E-02 mils per year (tank 241-AY-101) to 8.61E-02 mils per year (tank 241-AZ-102).

RPP-RPT-34697, Rev. 0

1. INTRODUCTION

The double-shell tanks (DST) are required to remain in service well beyond their design life to support the mission for treatment and disposal of the radioactive chemical wastes stored in the underground tank farms. To ensure the DSTs remain available for interim storage prior to Waste Treatment and Immobilization Plant (WTP) startup and during feed staging and transfer to support the WTP operations, the integrity of the DSTs must be protected. Controlling aggressive forms of corrosion helps to protect the integrity of the tanks and extend their useful life. The primary means for determining the impact of corrosion on the DSTs is to periodically perform ultrasonic examinations of the primary tank carbon steel wall. The corrosion rates determined from this method require measurements over long time periods. Another independent method for determining corrosion rates of carbon steel exposed to an electrolyte is by using electrochemical methods, which have the advantage of measuring a corrosion rate in a single measurement and nearly instantaneously.

Corrosion rates were determined using electrochemical methods for DSTs 241-AW-103 (AW-103), 241-AZ-102 (AZ-102), 241-AN-106 (AN-106), 241-AN-107 (AN-107), 241-AY-101 (AY-101), and 241-AY-102 (AY-102). Corrosion rates of the carbon steel types used in construction of the respective DSTs on exposure to the actual waste were determined for both a supernatant sample and a settled solids sample. The supernatant wastes were from samples obtained at the surface of the waste in each tank and were tested under quiescent conditions. Samples at this location in a tank are more likely to contain dissolved oxygen absorbed from the ventilation air, which generally will cause increased corrosion rates. The settled solids from all the tanks except for tank AN-106 were from core segments at the bottom of the tanks where oxygen is less likely to be present because of isolation from the ventilation air at this location in the tank. Extrusion and testing of the solids samples were performed under anaerobic conditions for all the tanks except tank AY-101. The settled solids in tank AN-106 are from recent single-shell tank retrieval transfers from the 241-C Tank Farm and no core sample from the solids layer is available for testing.

Table 1 shows the substrate and class of steel by tank. Table 2 gives the identification of the core (or grab sample) and segment numbers tested for each tank.

Table 1. Tank Samples and Steel; X = Sample to be Run Under this Test Plan; Done = Samples Run Under Previous Test Plans.

Tank/Material	AW-103	AZ-102	AN-106	AN-107	AY-101	AY-102
Supernatant	X	X	X	X	X	X
Sludge/saltcake	X	Done	NA	Done	X	Done
Steel	A537 Class 1	A515 Grade 60	A537 Class 1	A537 Class 1	A515 Grade 60	A515 Grade 60

1

RPP-RPT-34697, Rev. 0

Table 2. Sample Identification by Tank.

Tank	AW-103	AZ-102	AN-106	AN-107	AY-101	AY-102
Supernatant	Core 320 Segment 1	Core 316 Segment 1	Grab Sample 6AN-07-01	Core 309 Segment 1	Core 325 Segment 1A	Core 318 Segment 1
Sludge/saltcake	Core 321 Segment 21R2	Core 313 Segment 19/19R1 and 19R3	N/A	Core 309 Segment 21R1 and 21R2	Core 325 Segment 16R1 and 16R2	Core 308 Segments 14R1 and 14R2

The electrochemical derived corrosion rates for tanks AZ-102 and AY 102 sludges were documented and reported in RPP-20910, *Electrochemical Corrosion Studies, Core 313 Segments 19/19R1 and 19R3, Tank 241-AZ-102*, and RPP-18399, *Electrochemical Corrosion Studies, Core 308, Segments 14R1 and 14R2, Tank 241-AY-102*, respectively. The corrosion rate scans for tank AN-107 saltcake were completed in August 2006.

Two tank steel coupons per tank waste sample were tested using an electrochemical cell design that allows interrogation of a different sample location for each coupon. All electrochemical scans were carried out at ambient hot cell temperature, which is approximately 25 °C (77 °F).

The electrochemical derived corrosion rate was calculated from the cathodic and anodic Tafel slopes using "The Shape of Electrochemical Polarization Curves" equation (Stern and Geary 1957). The software associated with the slope data selection and the corrosion rate calculation is PowerCORR®,[1] which is also the potentiostat controlling software. The algorithm follows the ASTM®[2] G102-89 method, *"Standard Practice for Calculation of Corrosion Rates and Related Information from Electrochemical Measurements."*

The measured corrosion rates for tank AZ-102 supernatant and sludge are believed to also closely reflect the expected corrosion rates for tank 241-AZ-101 (AZ-101) because the waste from both tanks have the same origin. The waste in the tanks is classified as neutralized current acid waste, which was generated from caustic neutralization of the first cycle solvent extraction acid waste during the Plutonium Uranium Recovery Extraction Plant operations. Although there is variability between the supernatant compositions between the tanks, the wastes are highly alkaline at pH >13 and have high nitrite to nitrate ion concentration ratios, both of which are conducive to low corrosion rates.

2. TESTING PROTOCOL

2.1 TEST COUPONS (WORKING ELECTRODE)

Test carbon steel coupons were obtained from Metal Samples®,[3] and the geometry used for corrosion rate determination is shown in Figure 1. The coupons are supplied wrapped in corrosion-inhibited paper with a protective coating to keep oxygen from the surface. To prepare a coupon for use, the surface is sanded with 600-grit wet/dry sandpaper, placed in an organic

---

[1] PowerCORR® is a registered trademark of Advanced Measurement Technologies, Inc. Oak Ridge, Tennessee.
[2] ASTM® is a registered trademark of ASTM International, West Conshohocken, Pennsylvania.
[3] MetalSamples® is a division of Alabama Specialty Products, Munford, Alabama.

RPP-RPT-34697, Rev. 0

solvent (usually acetone or hexane), and sonicated for 2 minutes. It is then threaded onto a steel rod that has an insulating glass sleeve. Surgeon's gloves are worn when preparing the coupon to minimize contamination of the coupon surface. The coupons were prepared immediately before introduction into the sample and, once inserted, were allowed to equilibrate for a minimum of 18 hours.

Figure 1. Test Coupon Configuration.
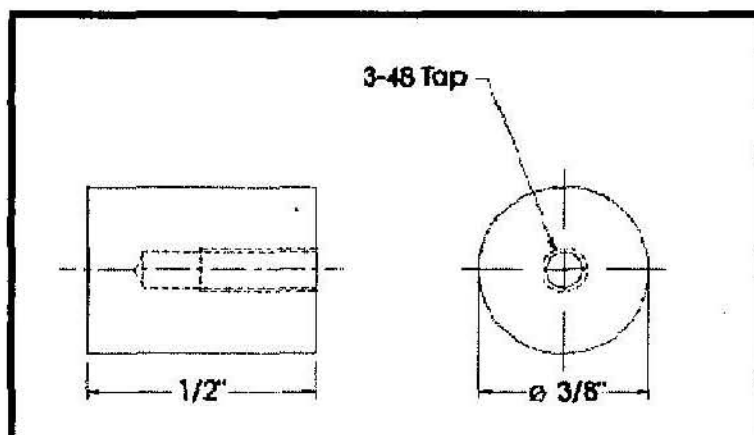
2.2 TEST CELL

Test samples were transferred to an I-CHEM[®][4] 500-mL sample jar. A lid, such as one shown in Figure 2, was secured to the sample jar. Note the argon gas inlet and outlet ports used to maintain anaerobic conditions in the test cell, when required. The carbon steel test coupon was placed in the working electrode port. Two high-density carbon rods were used as the counter electrodes, and a Luggin bridge filled with 1 $\underline{M}$ potassium nitrate was used to protect the reference electrode. The reference electrode is a Radiometer[®5] Model Number B20B110 saturated calomel electrode (SCE).

2.3 EXTRUSION STAND

To maintain anaerobic conditions for saltcake or sludge extrusion from the segment sampler, a test stand was constructed to allow the I-CHEM sample jar/electrochemical cell to receive the sample under argon gas purge. Figure 3 shows the extrusion stand with a segment sampler in position. The extrusion is carried out under LO-160-104, "Core Segment Extrusion Process by Push Mode Extruder."

---

[4] I-CHEM Certified is a registered trademark of I-CHEM Acquisition Co. Corporation, New Castle, Delaware.
[5] Radiometer is a registered trademark of Radiometer Analytical S.A., Lyon, France.

3

RPP-RPT-34697, Rev. 0

Figure 2. Electrochemical Cell Lid.

Argon Gas Inlet

Reference Electrode Port

Argon Gas Outlet

Thermocouple Port
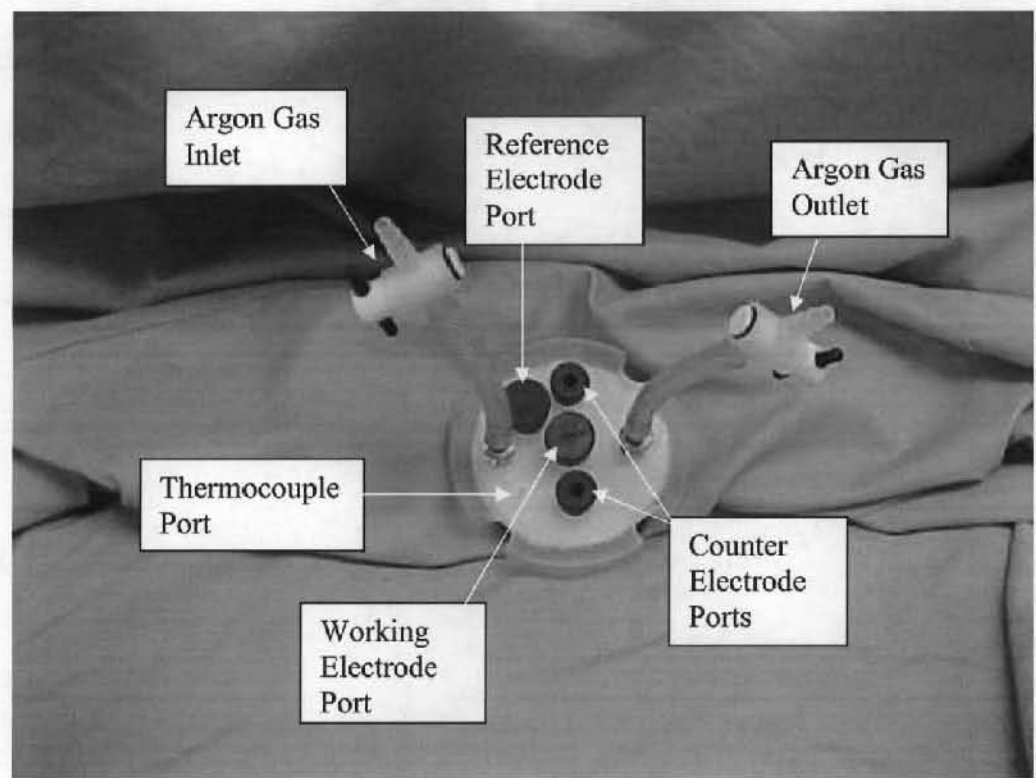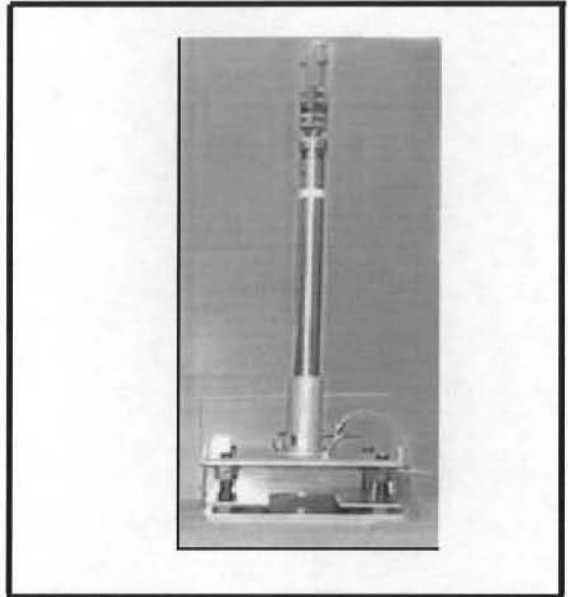
Working Electrode Port

Counter Electrode Ports

Figure 3. Anaerobic Extrusion Stand.

4

RPP-RPT-34697, Rev. 0

The oxygen is monitored using an oxygen deficiency meter. The meter used was an SMC[6] Model 55 with an external sensor (55-01). The unit was claimed to be able to record zero percent on the display; however, in reality it would achieve 0.3%. On consultation with Sierra Monitor Corporation personnel, an experiment was performed to ensure that when the meter read 0.3% on the scale, no oxygen was present in the container. This was achieved by designing an enclosure that could be purged with pure argon gas to create an anaerobic environment and checking the meter response with the sensor inserted in the oxygen free enclosure. The meter was then used to monitor the oxygen depletion in the extrusion stand during extrusion of the tank AW-103 segment.

The initial tank AY-101 segment extrusions were performed under anaerobic conditions using argon gas to purge oxygen from the sample jar/electrochemical cell and inside of the extrusion stand. However, complications during the extrusions with hydrostatic-head fluid (HHF) entrainment resulted in exposing portions of the sludge to be used in the testing to atmospheric air to recover enough sludge free of hydrostatic-head fluid contamination. A composite of the recovered sludge from Segments 16R1 and 16R2 was prepared in the sample jar/electrochemical cell and purged with argon to remove oxygen from the cell headspace. The measured corrosion rate for the composite sample is expected to be conservative since any oxygen absorbed by the sample from exposure to the air will generally cause increased corrosion rates.

For those tank segments extruded previously, tanks AN-107, AY-102, and AZ-102, a Matheson-Trigas[®7] Model 8061 oxygen deficiency meter was used. This model did register 0.0% oxygen. The model is no longer manufactured.

2.4 POTENTIOSTAT

A PARSTAT[®8] 2263 with data collection and analyses software, PowerSuite[®9] advanced electrochemistry software, was used to subject the coupons to electrochemical corrosion scans. The PARSTAT[®] 2263 has a compliance voltage of 20 V (power available at the counter electrode) and a maximum current of 200 mA.

2.5 QUALITY CONTROL

ASTM G5-94, *Standard Reference Test Method for Making Potentiostatic and Potentiodynamic Anodic Polarization Measurements*, is run before and after electrochemical corrosion scans. The current density acquired during the run in the hot cell is plotted against the reported current densities in the ASTM G5-94 publication. Figure 4 shows response by the I-CHEM[®] sample jar/electrochemical cell as compared to the ASTM G5-94 results from the round robin potentiodynamic test project that yielded the published scatter bands included in Figure 4. The before-and-after scan values for the test equipment configuration are essentially the same and compare very closely with the ASTM results.

---

[6] SMC Model 55 oxygen deficiency meter is a product of Sierra Monitor Corporation, Milpitas, California.
[7] Matheson-Trigas is a registered trademark of Matheson Gas Products, Valley Forge, Pennsylvania.
[8] PARSTAT is a registered trademark of Princeton Applied Research, Oak Ridge, Tennessee.
[9] PowerSuite is a registered trademark of Advanced Measurement Technology, Inc., Oak Ridge, Tennessee.

5

RPP-RPT-34697, Rev. 0

Figure 4. I-CHEM Electrochemical Cell Response to the ASTM G5-94 Method.
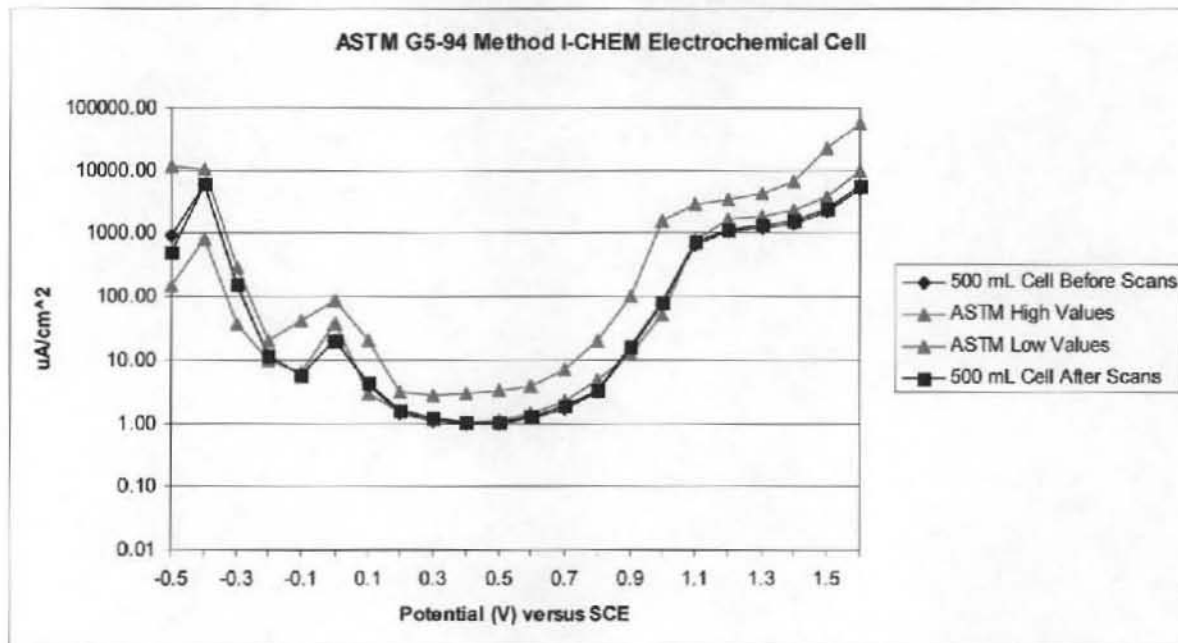
2.6 SUPERNATANT

Supernatant from tanks AN-106, AN-107, AW-103, AY-101, AY-102, and AZ-102 were received and scanned without argon purge. The samples were decanted into the sample jar/electrochemical cell, and coupons were scanned after equilibrating for at least 18 hours. After the scans were completed, the sample was decanted back into the archive jar, the cell was thoroughly washed with deionized water, and allowed to air dry before the next sample was introduced into the sample jar/electrochemical cell.

With the exception of tank AN-107, all supernatant was straw colored in appearance. The appearance of tank AN-107 supernatant was black in color.

2.7 SALTCAKE

As mentioned in Section 1, this test scope required two tanks to be extruded, tanks AW-103 and AY-101, to recover material for the electrochemical testing as described in RPP-20910 and RPP-18399, respectively. Similar testing on tank AN-107 saltcake waste has been completed and the results are documented as part of this work.

The solids in tank AY-101 behave as a dilatant fluid, much like wet sand. This material behavior presented difficulties during the extrusion process. A partial anaerobic extrusion of Core 325, Segment 16R2, yielded HHF co-mingled with the portion of sludge that was extruded. The HHF is composed of lithium bromide and is not a compound found in the waste tanks from Hanford

6

RPP-RPT-34697, Rev. 0

processes. A decision was made to abandon the vertical extrusion of Segment 16R2 due to contamination of the sludge with HHF and collect the remainder of the sludge segment using an aerobic horizontal extrusion process. This extrusion produced sludge that appeared to be free from HHF contamination. Segment 16R1 was also vertically extruded. Although some HHF was observed to flow into the cell during extrusion, a pillar of sludge standing upright in the sample jar was not in contact with the fluid in the bottom. The upright cylinder of sludge was carefully recovered aerobically from the jar to minimize exposure to the HHF. This sample material was mixed with the material from the horizontal extrusion of Segment 16R2. The composite sample was placed under argon and used for electrochemical corrosion scans.

2.7.1 Tank 241-AN-107 Saltcake

Tank 241-AN-107 was core sampled (Core 309) between June 19, 2003, and August 4, 2003. During the Core 309 sampling event, two Segment 21 retakes were obtained from the waste at the bottom of the tank for electrochemical corrosion testing. The electrochemical testing took place under RPP-PLAN-29001, *Electrochemical Corrosion Studies for Tank 241-AN-107, Core 309, Segments 21R1 and 21R2*. Electrochemical scans were performed on the interstitial liquid (Segment 21R1) and the saltcake (Segment 21R2).

Segment 21R1 was horizontally extruded and the solids were transferred to centrifuge cones and centrifuged for 24 hours. Approximately 60 mL of interstitial liquid was recovered. The interstitial liquid was transferred to a 125 mL I-CHEM® glass jar which served as the electrochemical test cell. Electrochemical scans were performed under quiescent conditions (i.e., no inert gas sparging to displace oxygen in the sample) on the interstitial liquid

The Segment 21R2 saltcake was vertically extruded (~260 mL) under anaerobic conditions into a 500 mL I-CHEM® glass jar, which served as the electrochemical test cell. The test cell was kept under a sweep of humidified argon gas during the electrochemical corrosion testing.

2.7.2 Tank 241-AW-103 Saltcake and Tank 241-AY-101 Sludge

Tank AW-103 was extruded without incident and yielded a grayish colored moist sample.

The solids in tank AY-101 behave as a dilatant fluid, much like wet sand. Since the electrochemical cells used for the interstitial liquid and saltcake had different sample volumes, two ASTM G5-94 standard scans were performed to confirm the performance of the electrochemical system and ensure the electrodes and potentiostat instrument were functioning properly prior to testing the actual waste samples. The standard scans for the two electrochemical cells are shown in Figures 5 and 6. The scan values for the two test equipment configurations compare very closely with the ASTM results.

RPP-RPT-34697, Rev. 0

Figure 5. ASTM Scan using a 125 mL I-CHEM Electrochemical Cell.
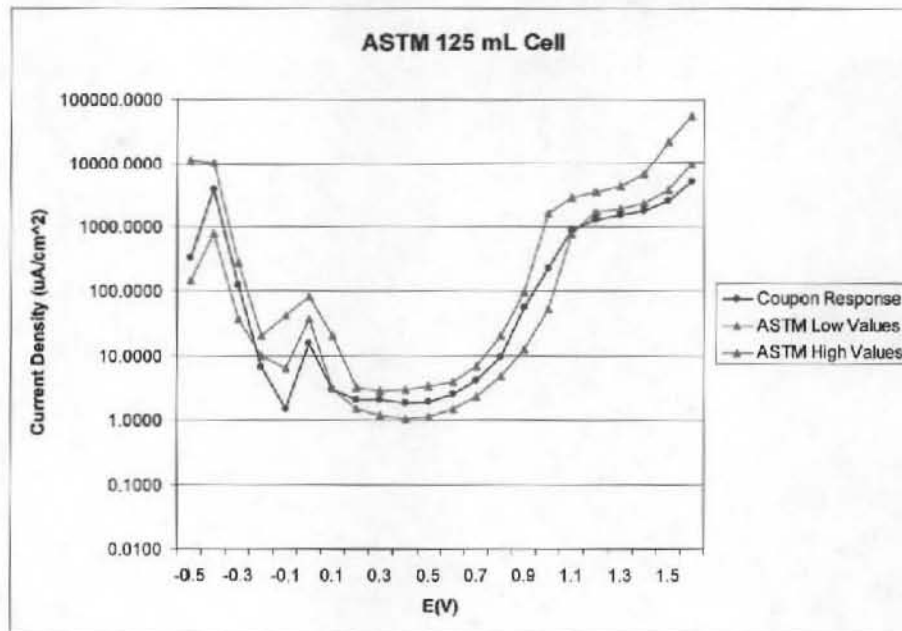
Figure 6. ASTM Scan using a 500 mL I-CHEM Electrochemical Cell.
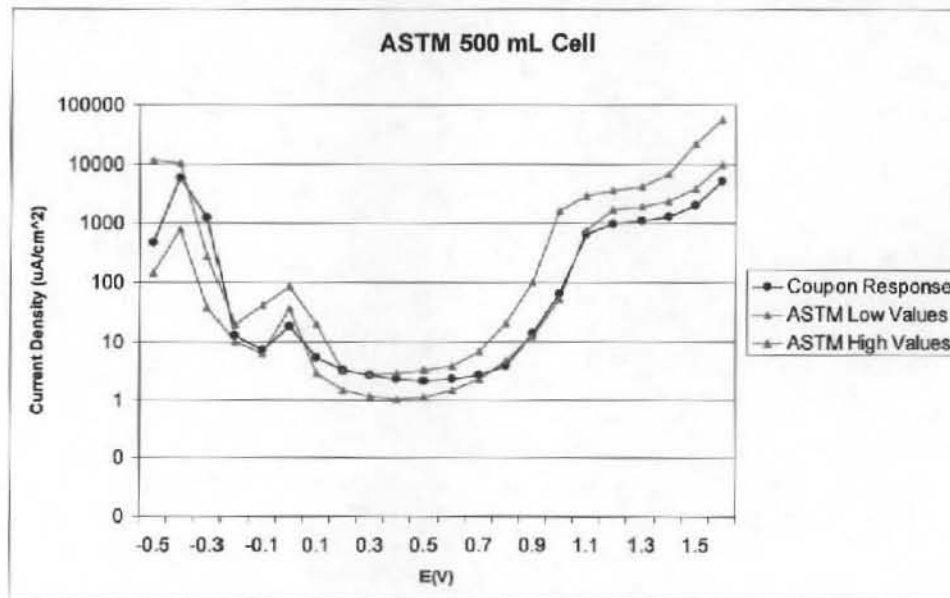
3. RESULTS

Table 3 shows the results of the supernatant electrochemical corrosion scans. Table 4 gives the results for the solids samples. As can be determined, the corrosion rate for all coupons was less than 1 mpy. The chi-square statistic is less than 100 for each Tafel fit, which indicates the goodness of fit for the data were acceptable, and therefore the parameters of the scan were acceptable.

8

RPP-RPT-34697, Rev. 0

Table 3. Supernatant Electrochemical Corrosion Scan Results.

Tank 241-	OCP (mV)	i_{CORR} (µA)	Corrosion Rate (mpy)	χ^{2a}
AY-102				
Coupon 1	-240.1	2.17E-01	1.7E-02	15.87
Coupon 2	-252.2	2.65E-01	2.075E-02	8.66
AY-101				
Coupon 1	-281.5	2.11E-01	1.65E-02	53.57
Coupon 2	-240.8	1.77E0	1.39E-01	1.93
AW-103				
Coupon 1	-314.6	6.99E-02	5.47E-03	0.25
Coupon 2	-300.7	7.00E-02	5.48E-03	0.27
AN-107				
Coupon 1	-379.8	2.76E-01	2.16E-02	1.68
Coupon 2	-370.7	4.75E-01	3.72E-02	0.55
AN-106				
Coupon 1	-337.7	5.33E-02	4.17E-03	0.11
Coupon 2	-220.7	1.88E-01	1.48E-02	0.09
AZ-102				
Coupon 1	-229.4	5.23E-02	4.1E-03	0.63
Coupon 2	-241.37	4.31E-02	3.37e-03	1.06

[a] $\chi^2 = \Sigma\, (i_{observed} - i_{expected})^2 / i_{expected}$

Table 4. Saltcake and Sludge Electrochemical Corrosion Rates.

Tank 241-	OCP (mV)	i_{CORR} (µA)	Corrosion Rate (mpy)	χ^{2a}
AW-103 (saltcake)				
Coupon 1	-586.1	3.19E-01	2.5E-02	11.38
Coupon 2	-576.2	2.52E-01	1.97E-02	8.50
AY-101 (sludge)[b]				
Coupon 1	-262.3	7.0E-02	5.49E-03	3.55
Coupon 2	-199.7	1.39E-01	1.1E-02	8.14
AY-102 (sludge)[c]				
Coupon 1	-430.8	1.4E-02	1.8E-03	41.13
Coupon 2	-255	2.3E-01	1.8E-02	9.37
AN-107 (saltcake)				
Coupon 1 (interstitial liquid)	-293.2	4.79E-02	3.61E-03	52.85
Coupon 2 (saltcake)	-347.1	1.4E-02	1.1E-03	56.40
AZ-102[d]				
Coupon 1	-233.7	1.1E-01	8.61E-03	8.75
Coupon 2	-237.1	9.0E-02	6.8E-03	29.97

[a] $\chi^2 = \Sigma\, (i_{observed} - i_{expected})^2 / i_{expected}$
[b] Composite of Segments 16R1 and 16R2 tested under aerobic conditions
[c] RPP-18399, *Electrochemical Corrosion Studies, Core 308, Segments 14R1 and 14R2, Tank 241-AY-102*
[d] RPP-20910, *Electrochemical Corrosion Studies, Core 313 Segments 19/19R1 and 19R3, Tank 241-AZ-102*

9

RPP-RPT-34697, Rev. 0

Appendix A contains scans for the supernatant, and Appendix B contains scans for the saltcake. Appendix C discusses the calculations involving the Tafel plot and the use of the corrosion current to obtain a corrosion rate in mils per year.

4.   CONCLUSIONS

Based on the Tafel scans and subsequent Stern-Geary calculations (Stern and Geary 1957), the corrosion rates were found to be less than 1 mpy for both the supernatant and solids samples from all the tanks using electrochemical measurement method employed in this testing project.

Because tanks AZ-101 and AZ-102 supernatant and sludge originated from the Plutonium Uranium Recovery Extraction Plant process and have similar waste characteristics, the electrochemical based corrosion rates for the neutralized current acid waste currently stored in the tanks are expected to be similar. Only waste samples from tank AZ-102 were available for this testing project. Therefore, the measured corrosion rate for tank AZ-102 from this work is likely reflective of the corrosion rate that would be expected for tank AZ-101.

5. REFERENCES

ASTM G5-94, 1999, *Standard Reference Test Method for Making Potentiostatic and Potentiodynamic Anodic Polarization Measurements*, Designation G5–94 (Reapproved 1999), American Society for Testing and Materials, West Conshohocken, Pennsylvania.

ASTM G102-89, 2004, *Standard Practice for Calculation of Corrosion Rates and Related Information from Electrochemical Measurement*, Designation G102-89 (Reapproved 2004), American Society for Testing and Materials, West Conshohocken, Pennsylvania.

LO-160-104, Rev F-0, "Core Segment Extrusion Process by Push Mode Extruder," Advanced Technologies and Laboratories International, Inc. Richland, Washington.

Princeton Applied Research, Queried 07/17/07, "Basics of Corrosion Measurements," Application Note CORR 1, Princeton Applied Research Applied Instruments Group, Oak Ridge, Tennessee. http://www.princetonappliedresearch.com/applications/application_notes/087.pdf

RPP-18399, 2003, *Electrochemical Corrosion Studies, Core 308, Segments 14R1 and 14R2, Tank 241-AY-102*, Rev. 0, CH2M HILL Hanford Group, Richland, Washington.

RPP-20910, 2004, *Electrochemical Corrosion Studies, Core 313 Segments 19/19R1 and 19R3, Tank 241-AZ-102*, Rev. 0, CH2M HILL Hanford Group, Richland, Washington.

RPP-PLAN-29001, 2006, *Electrochemical Corrosion Studies for Tank 241-AN-107, Core 309, Segments 21R1 and 21R2*, Rev. 0, CH2M HILL Hanford Group, Richland, Washington.

Stern, M., and A. L. Geary, 1957, "The Shape of Electrochemical Polarization Curves," *J. Electrochem. Soc.*, 104, 56.

RPP-RPT-34697, Rev. 0

APPENDIX A

Supernatant Tafel Scans

RPP-RPT-34697, Rev. 0

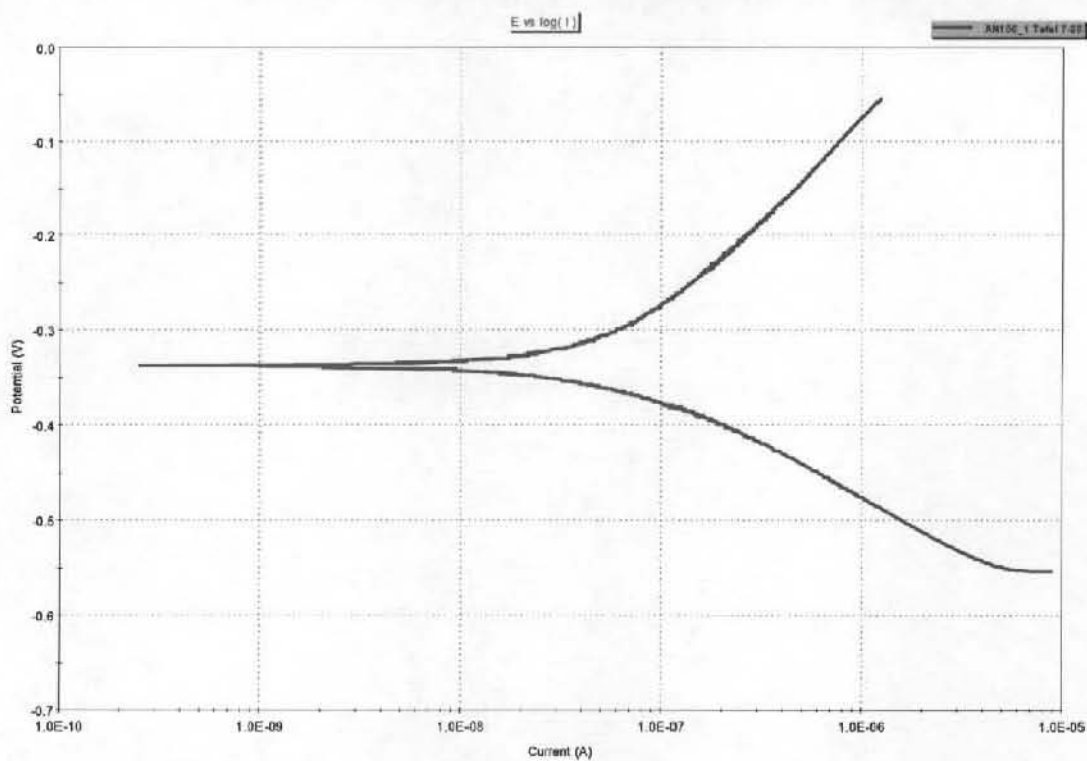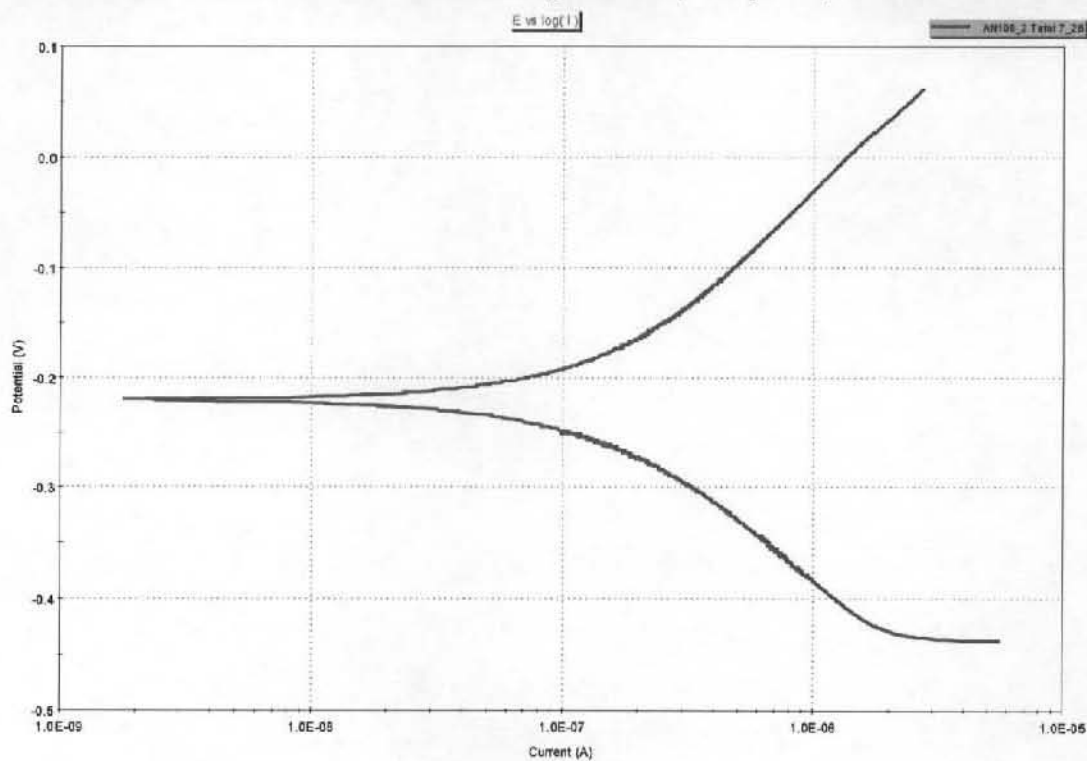**Figure A-1. Tafel Scan for Tank 241-AN-106 Supernatant, Coupon 1, Potential versus SCE.**

Figure A-2. Tafel Scan for Tank 241-AN-106 Supernatant, Coupon 2, Potential versus SCE.

A-1

RPP-RPT-34697, Rev. 0

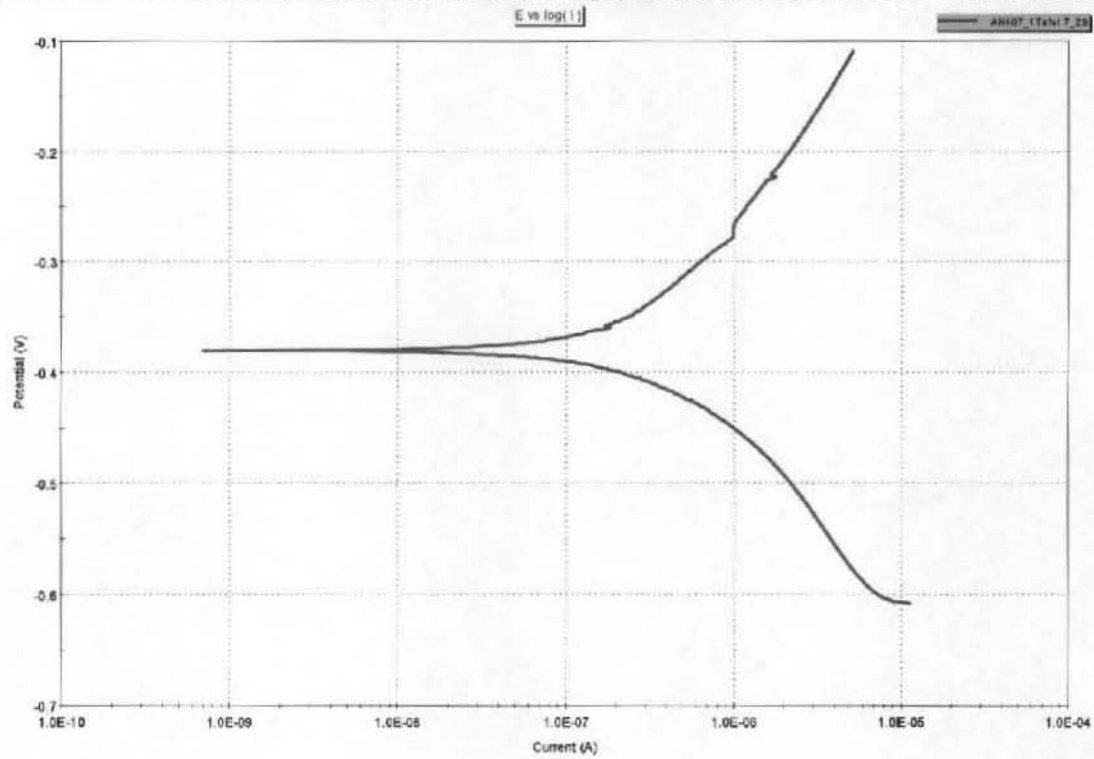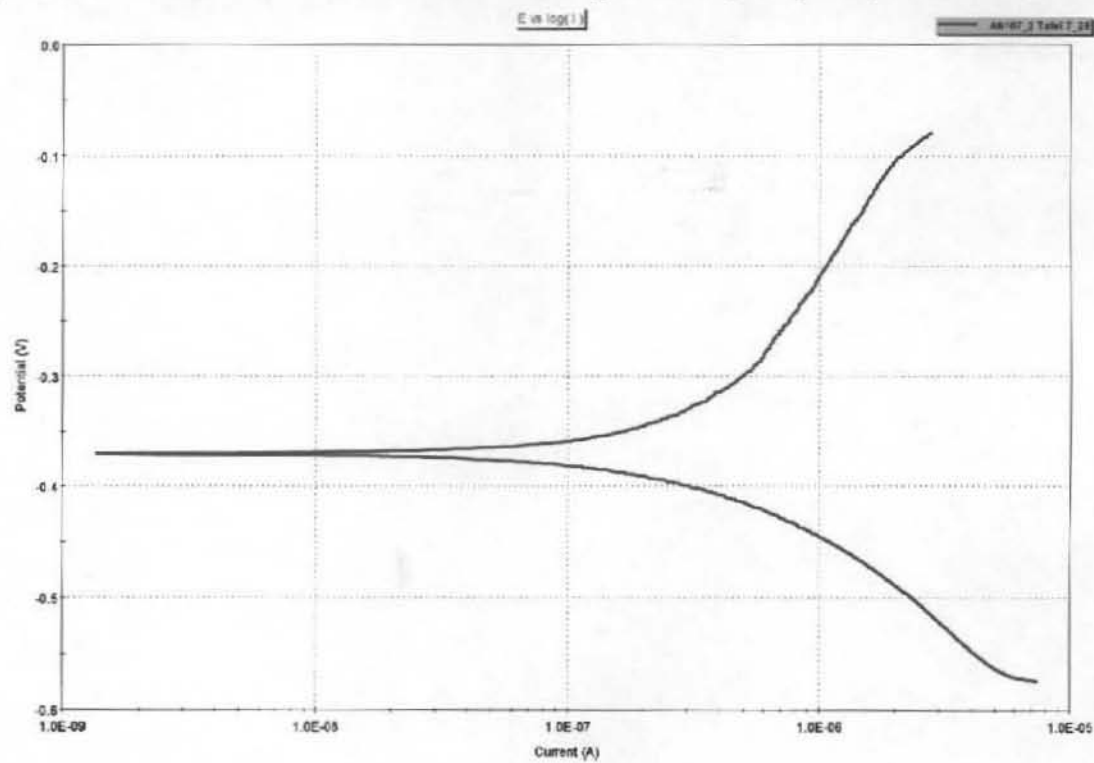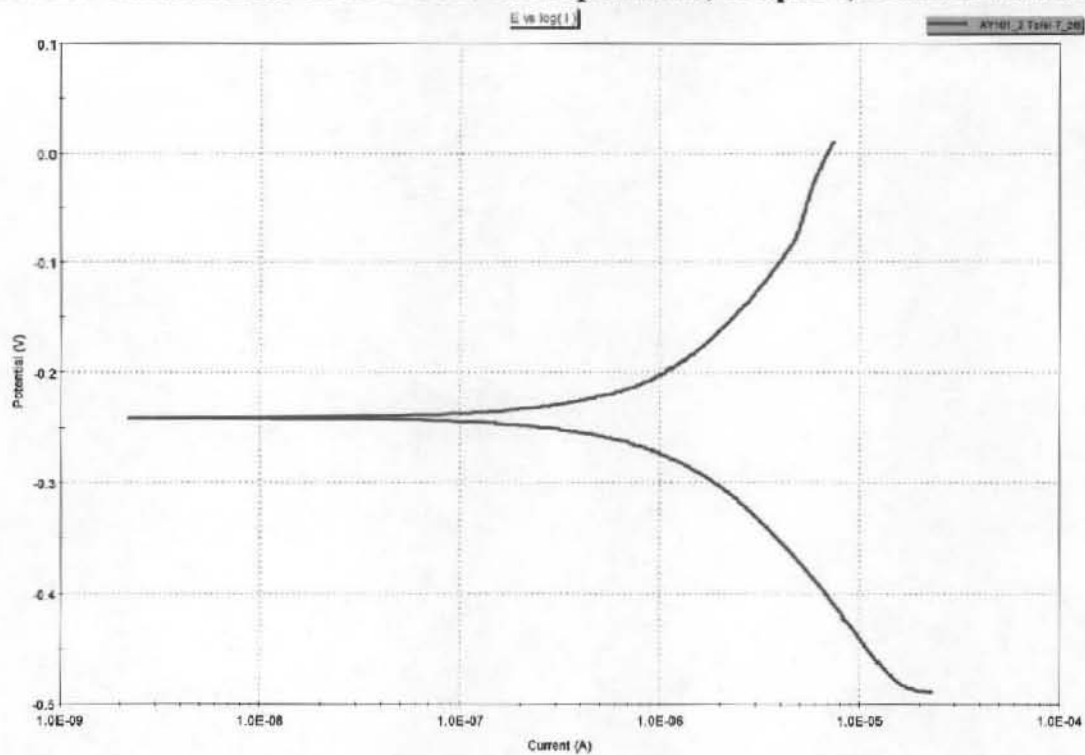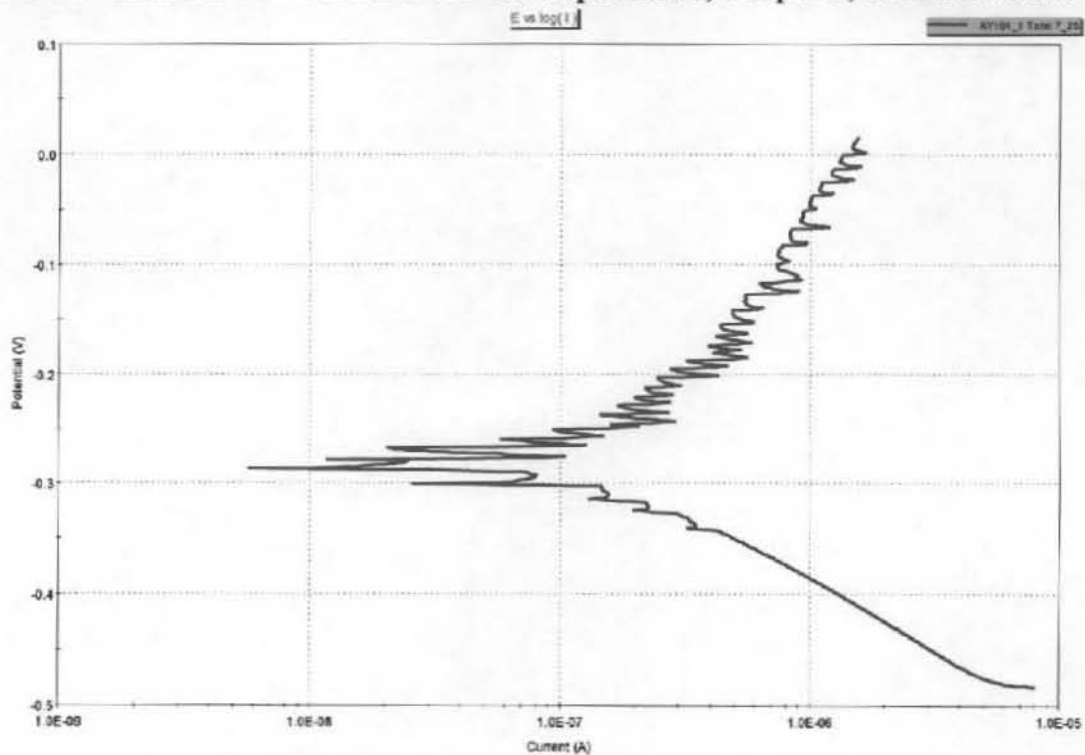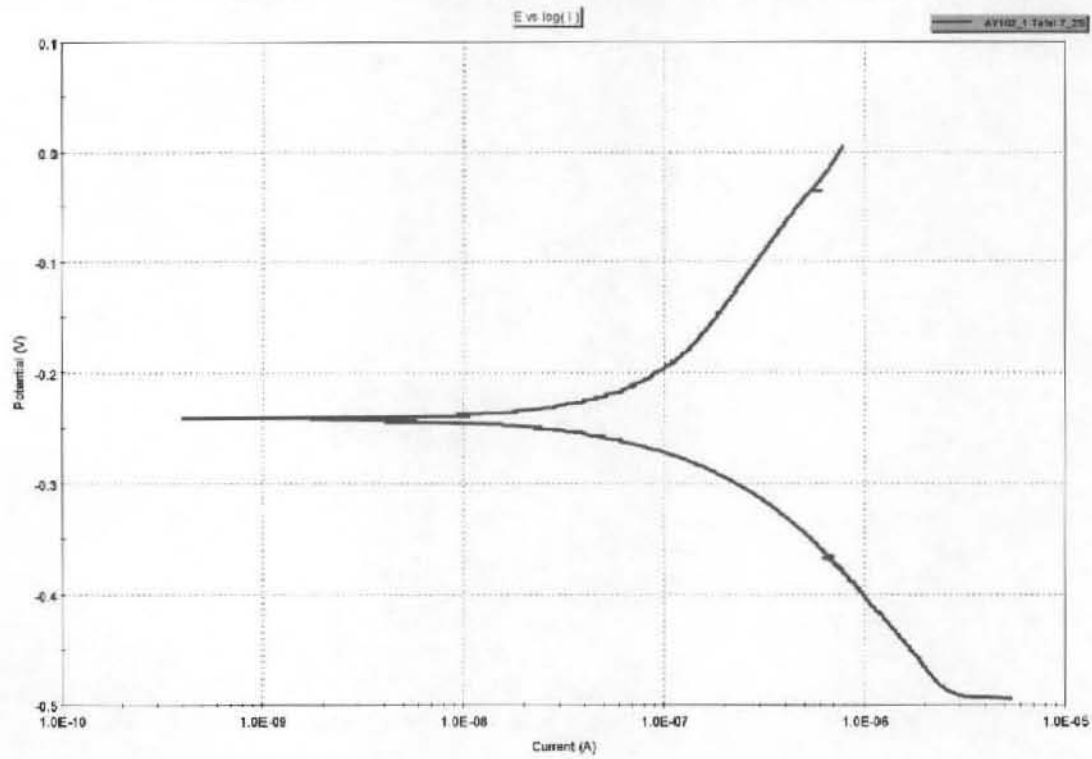**Figure A-3. Tafel Scan for Tank 241-AN-107 Supernatant, Coupon 1, Potential versus SCE.**
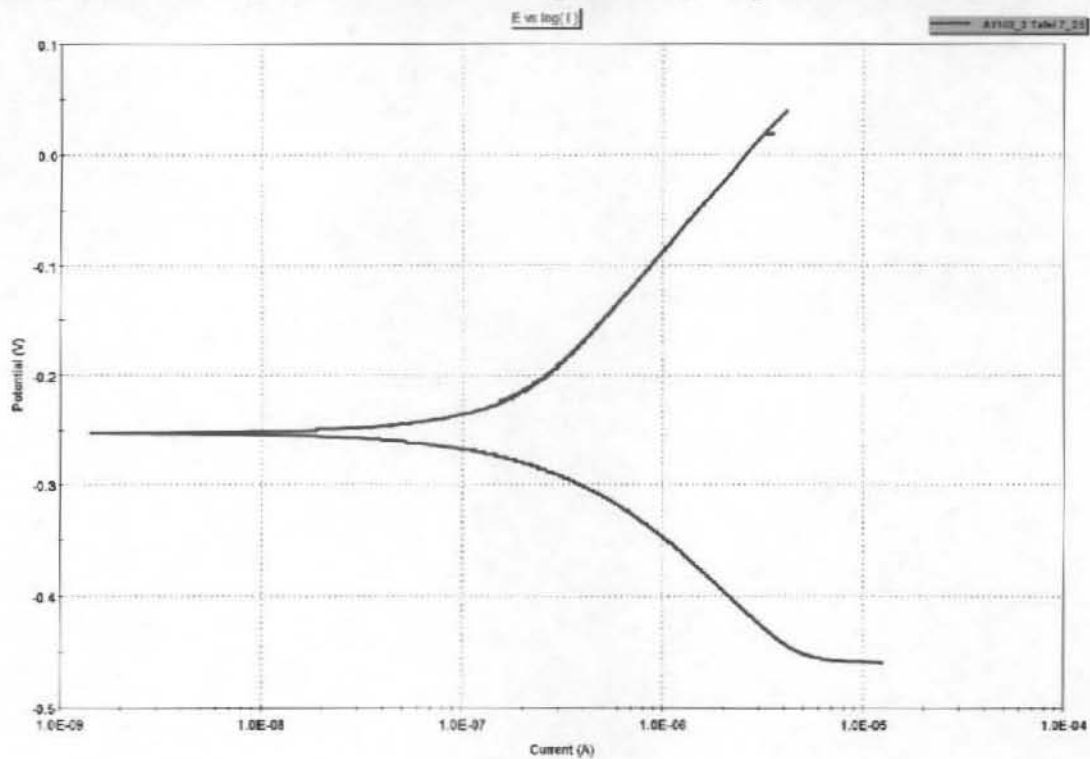

Figure A-4. Tafel Scan for Tank 241-AN-107 Supernatant, Coupon 2, Potential versus SCE.

A-2

RPP-RPT-34697, Rev. 0

Figure A-5. Tafel Scan for Tank 241-AY-101 Supernatant, Coupon 1, Potential versus SCE.
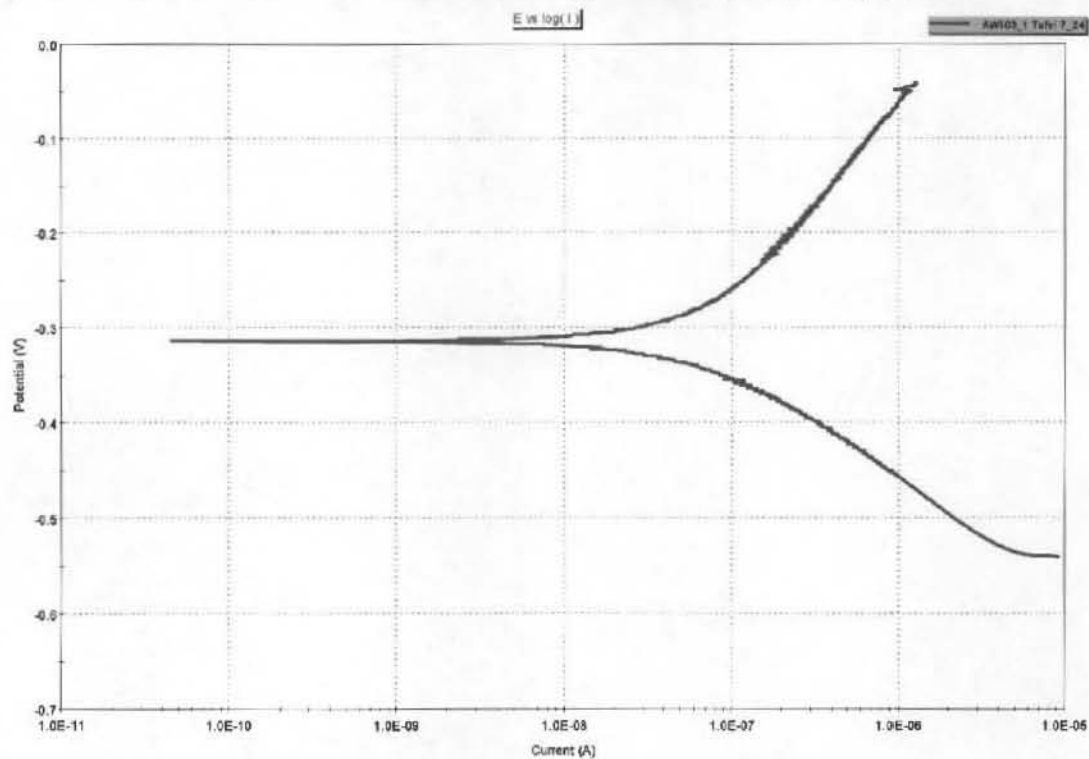

Figure A-6. Tafel Scan for Tank 241-AY-101 Supernatant, Coupon 2, Potential versus SCE.

A-3

RPP-RPT-34697, Rev. 0

Figure A-7. Tafel Scan for Tank 241-AY-102 Supernatant, Coupon 1, Potential versus SCE.
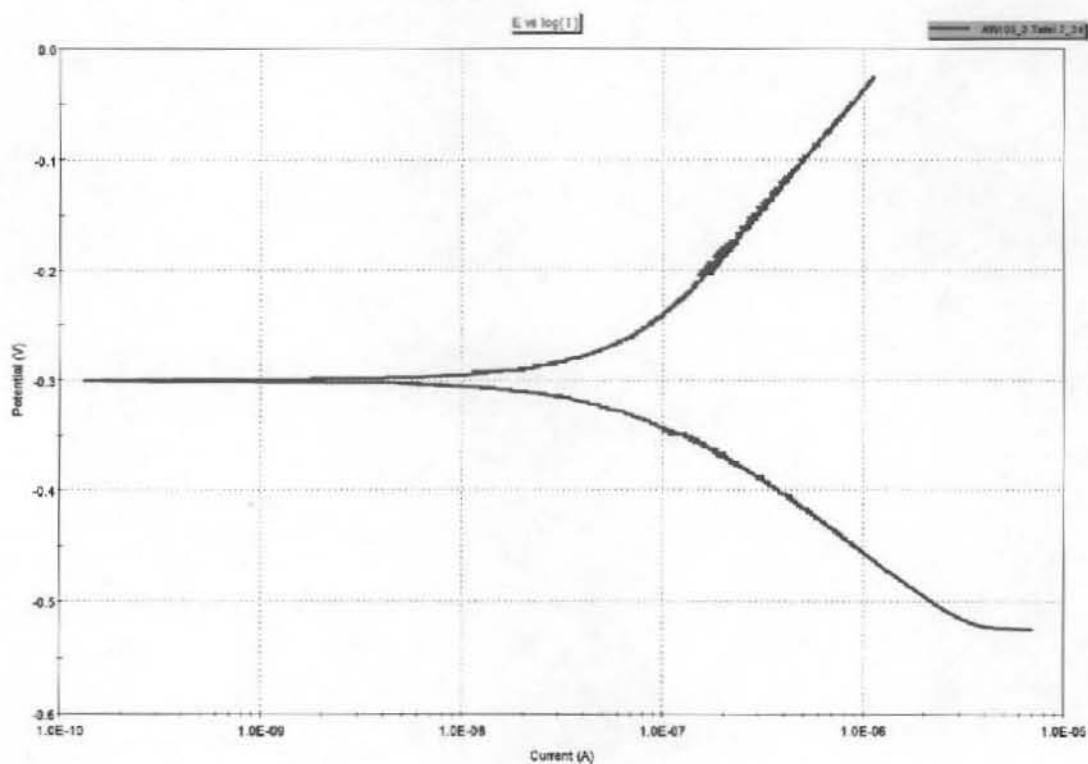

Figure A-8. Tafel Scan for Tank 241-AY-102 Supernatant, Coupon 2, Potential versus SCE.

A-4

RPP-RPT-34697, Rev. 0

Figure A-9. Tafel Scan for Tank 241-AW-103 Supernatant, Coupon 1, Potential versus SCE.

Figure A-10. Tafel Scan for Tank 241-AW-103 Supernatant, Coupon 2, Potential versus SCE.

A-5

RPP-RPT-34697, Rev. 0

Figure A-11. Tafel Scan for Tank 241-AZ-102 Supernatant, Coupon 1, Potential versus SCE.
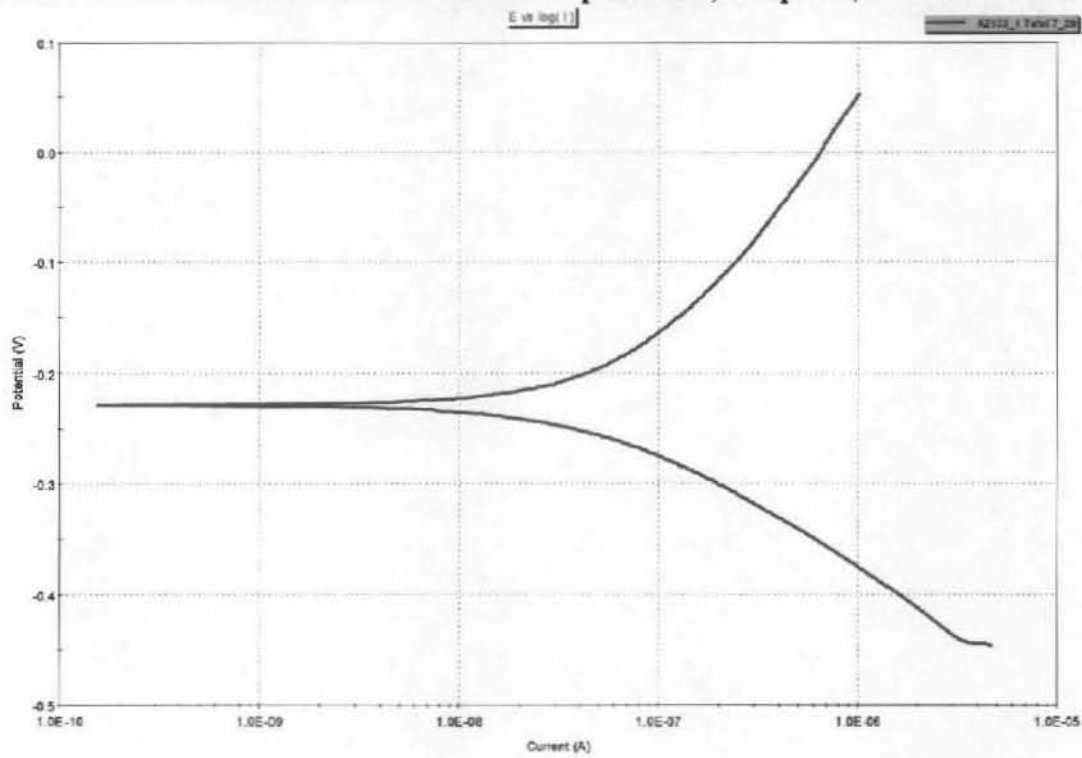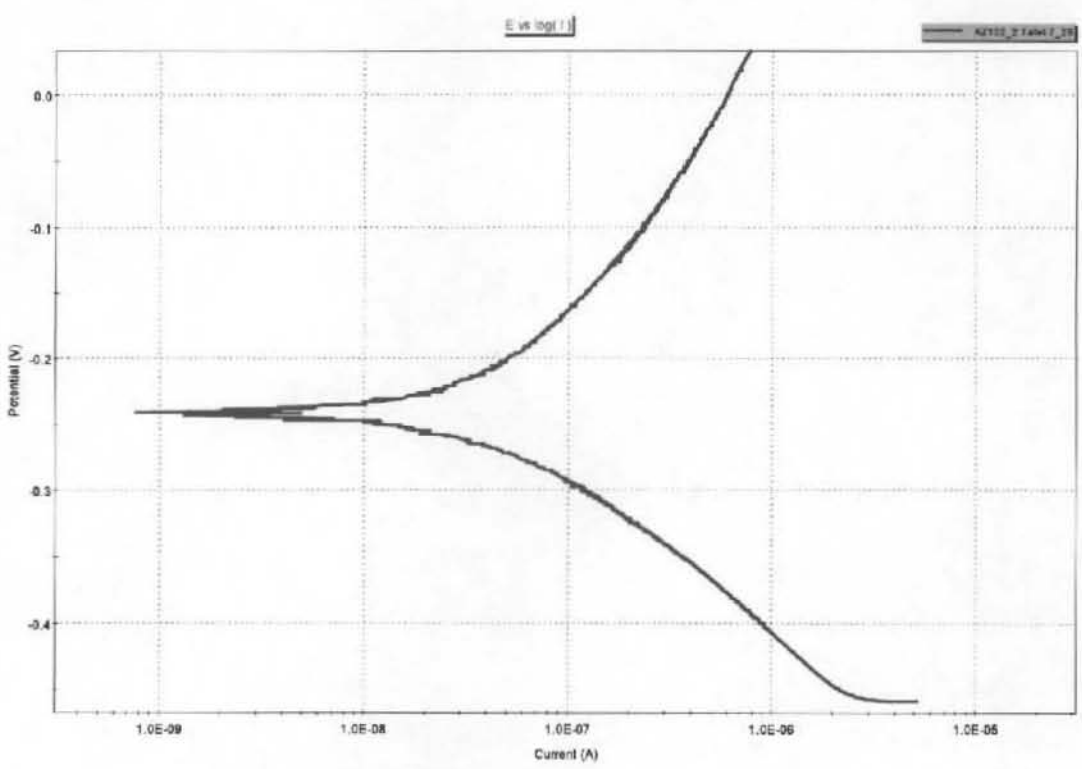

Figure A-12. Tafel Scan for Tank 241-AZ-102 Supernatant, Coupon 2, Potential versus SCE.

A-6

RPP-RPT-34697, Rev. 0

APPENDIX B

Saltcake and Sludge Tafel Scans

RPP-RPT-34697, Rev. 0

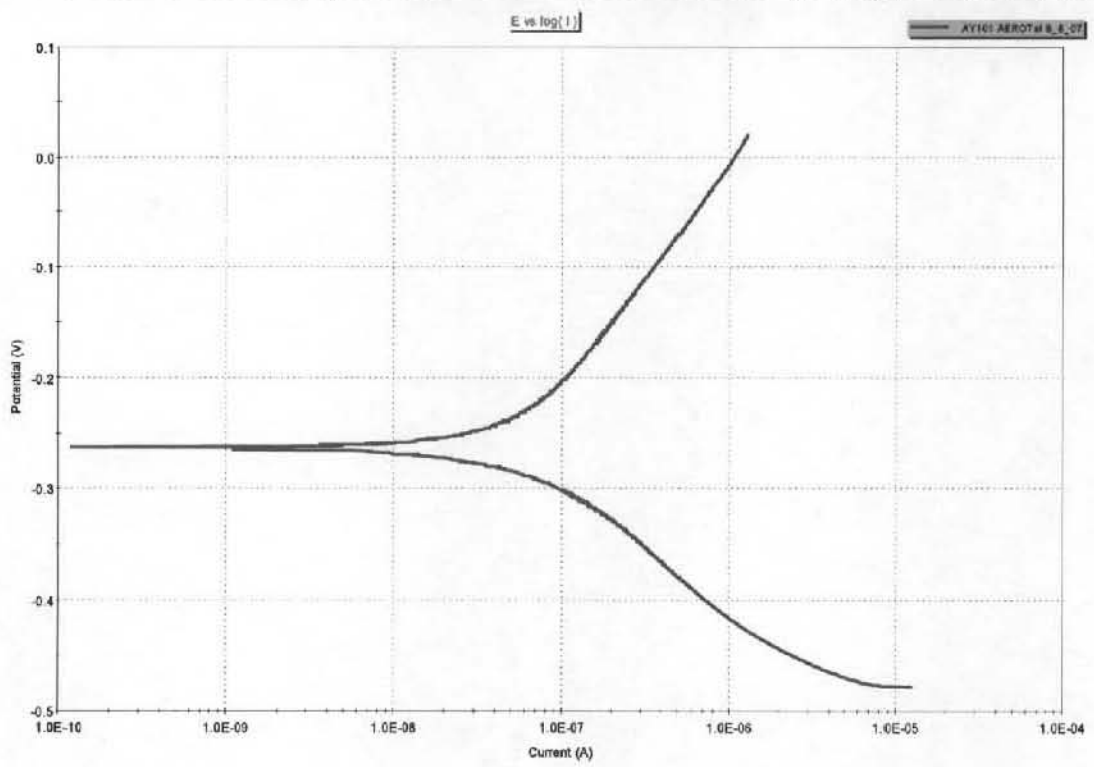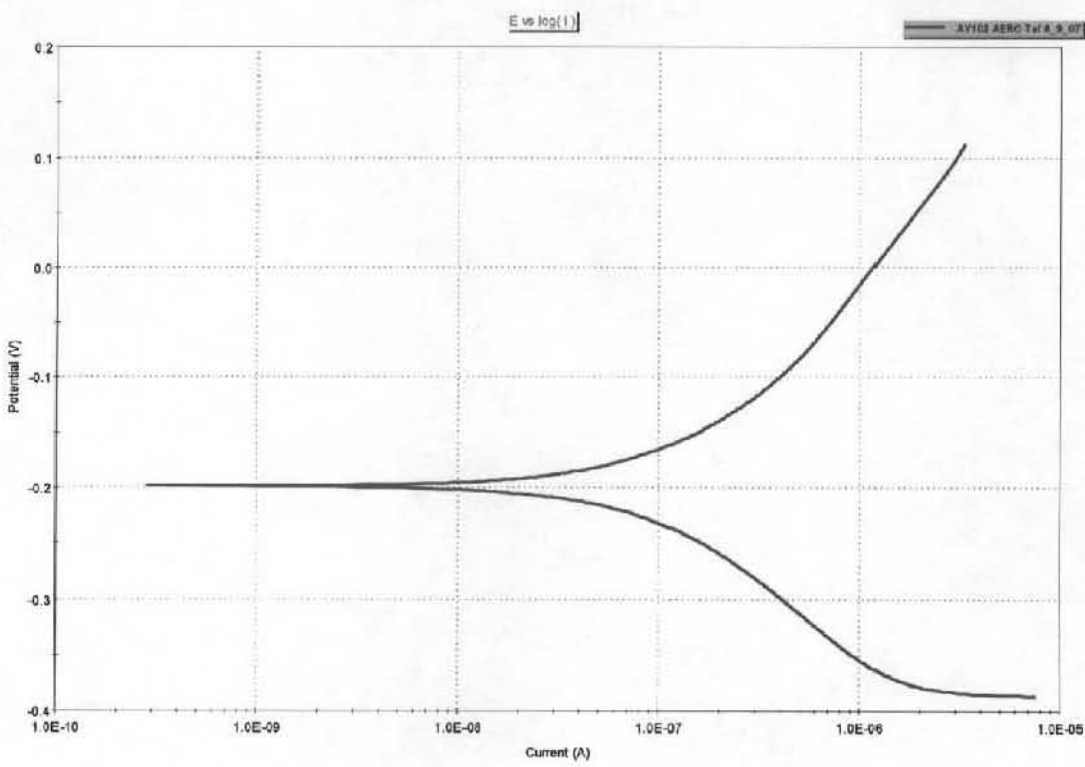**Figure B-1. Tank 241-AY-101, 16R1 and 16R2 Aerobic Extrusion, Sludge, Coupon 1, vs. SCE.**

Figure B-2. Tank 241-AY-101, 16R1 and 16R2 Aerobic Extrusion, Sludge, Coupon 2, vs. SCE.

B-1

RPP-RPT-34697, Rev. 0

Figure B-3. Tank 241-AW-103, Anaerobic Extrusion, Saltcake, Coupon 1, vs. SCE.
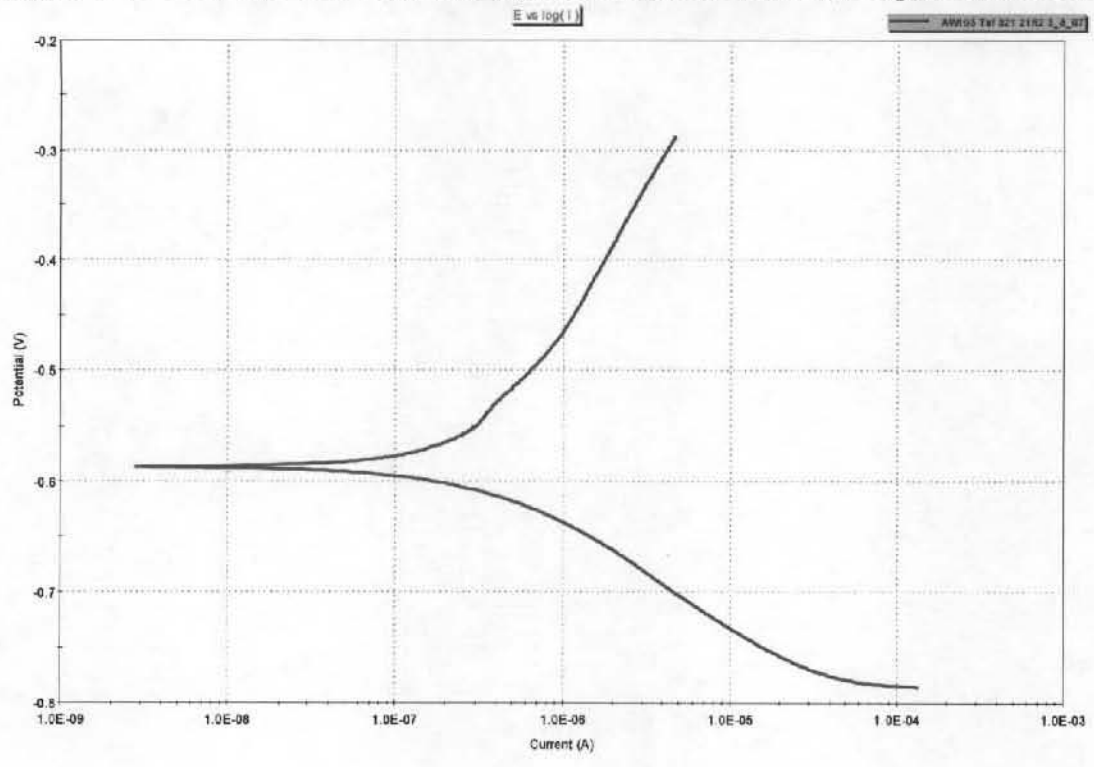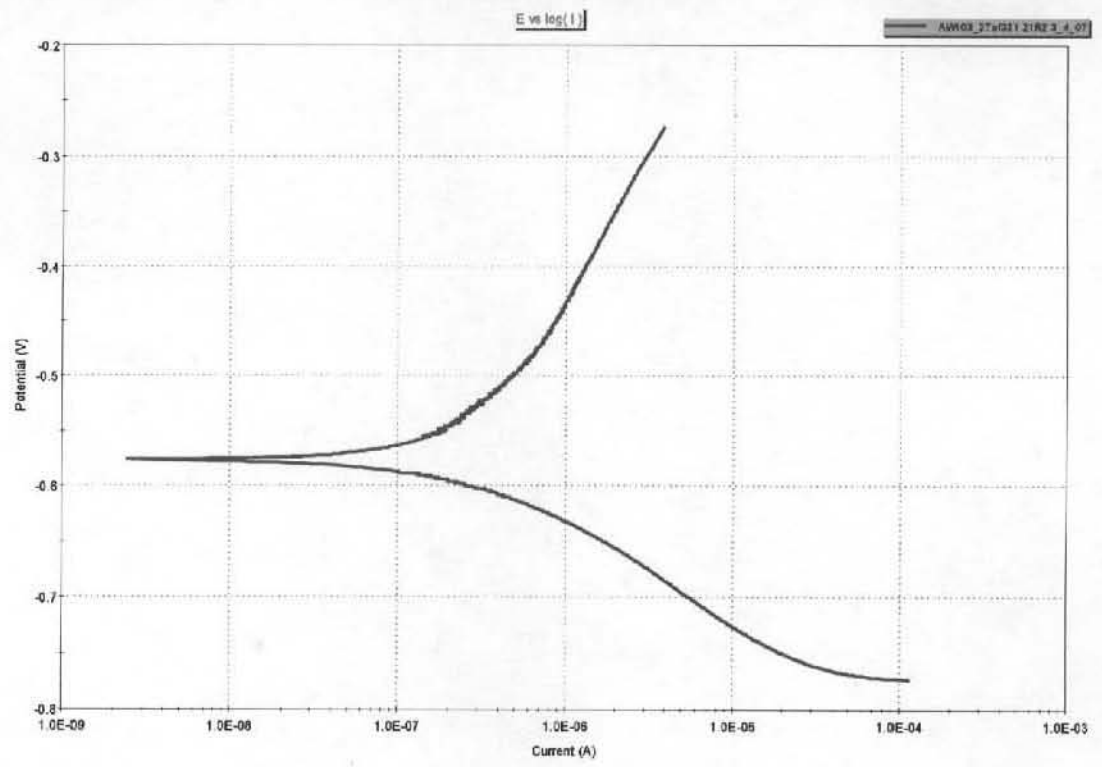

Figure B-4. Tank 241-AW-103, Anaerobic Extrusion, Saltcake, Coupon 2, vs. SCE.

B-2

RPP-RPT-34697, Rev. 0

Figure B-5. Tank 241-AZ-102, Anaerobic Extrusion, Sludge, Coupon 1 vs. SCE.

Figure B-6. Tank 241-AZ-102, Anaerobic Extrusion, Sludge, Coupon 2 vs. SCE.

B-3

RPP-RPT-34697, Rev. 0

Figure B-7. Tank 241-AY-102, Anaerobic Extrusion, Sludge, Coupon 1 vs. SCE.
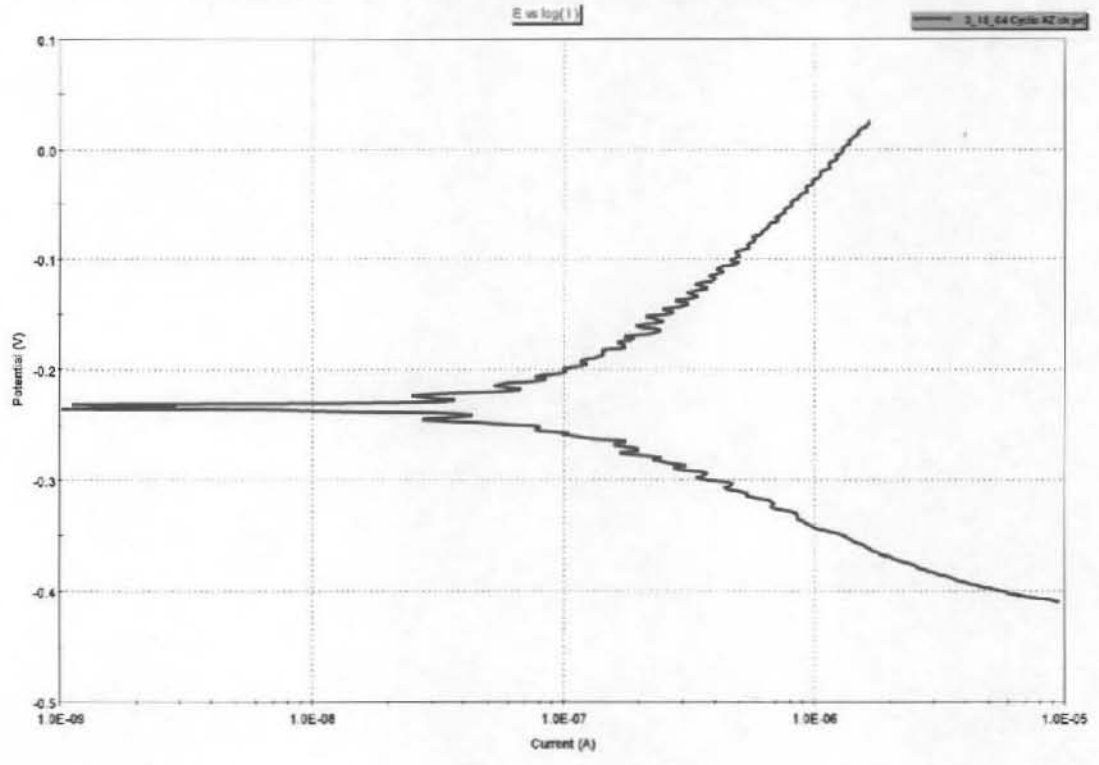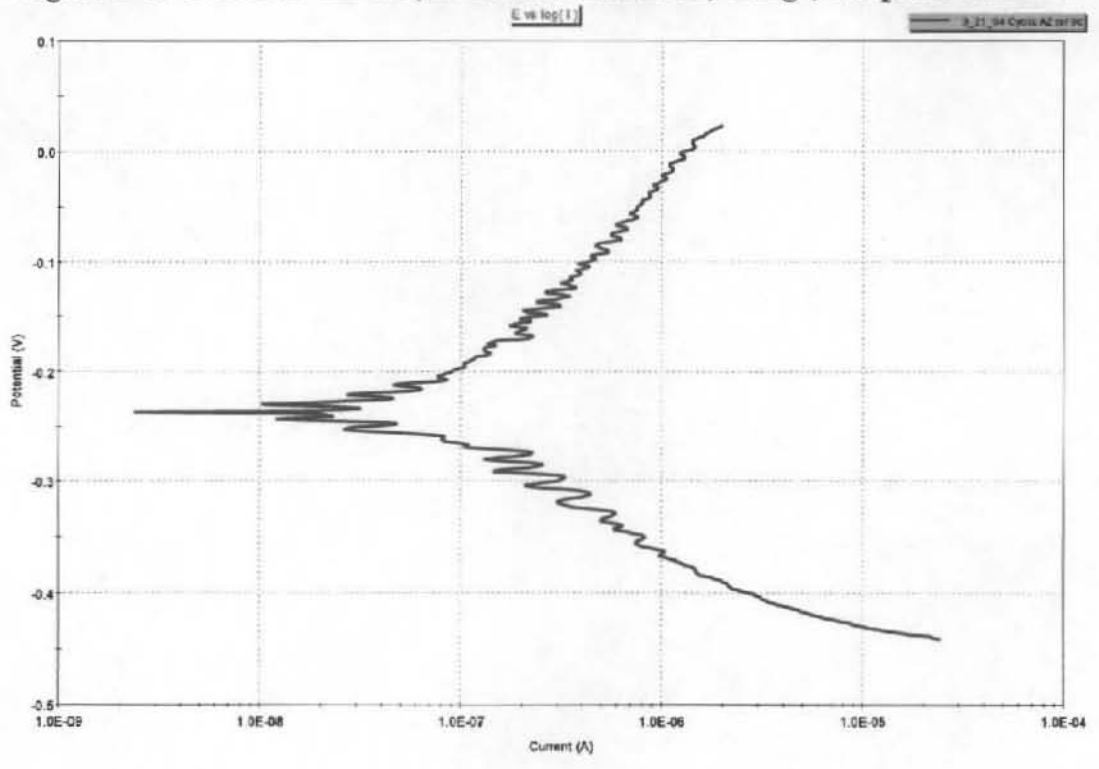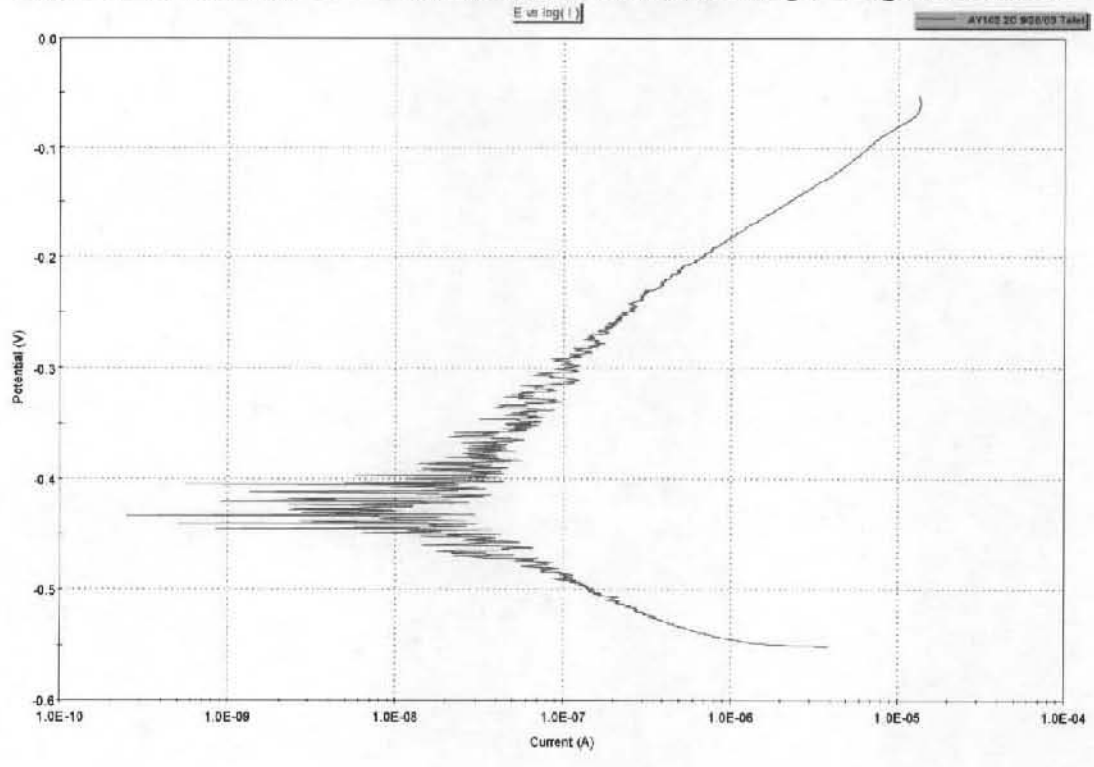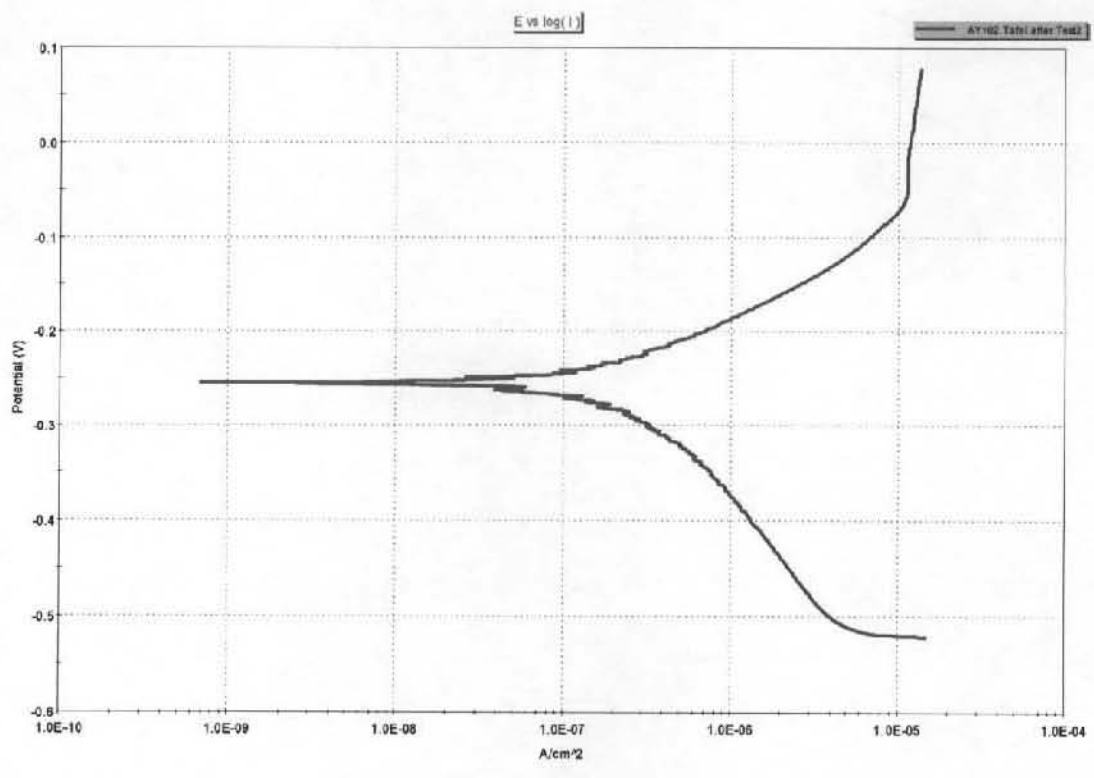

Figure B-8. Tank 241-AY-102, Anaerobic Extrusion, Sludge, Coupon 2 vs. SCE.

B-4

RPP-RPT-34697, Rev. 0

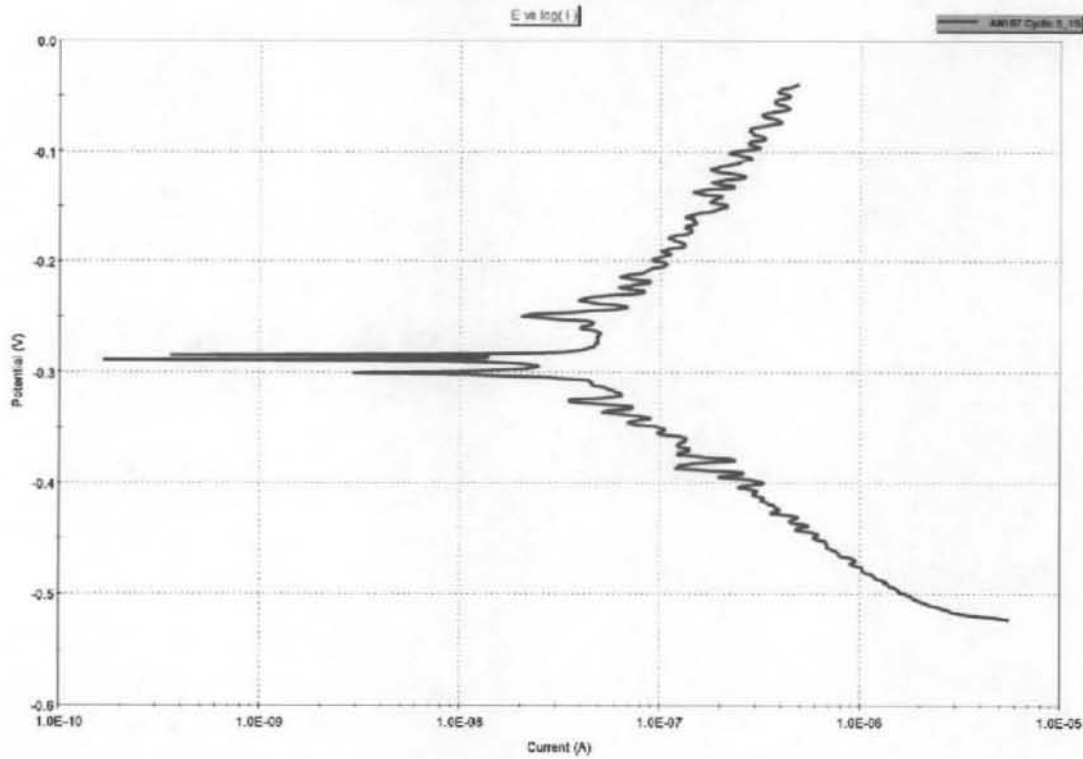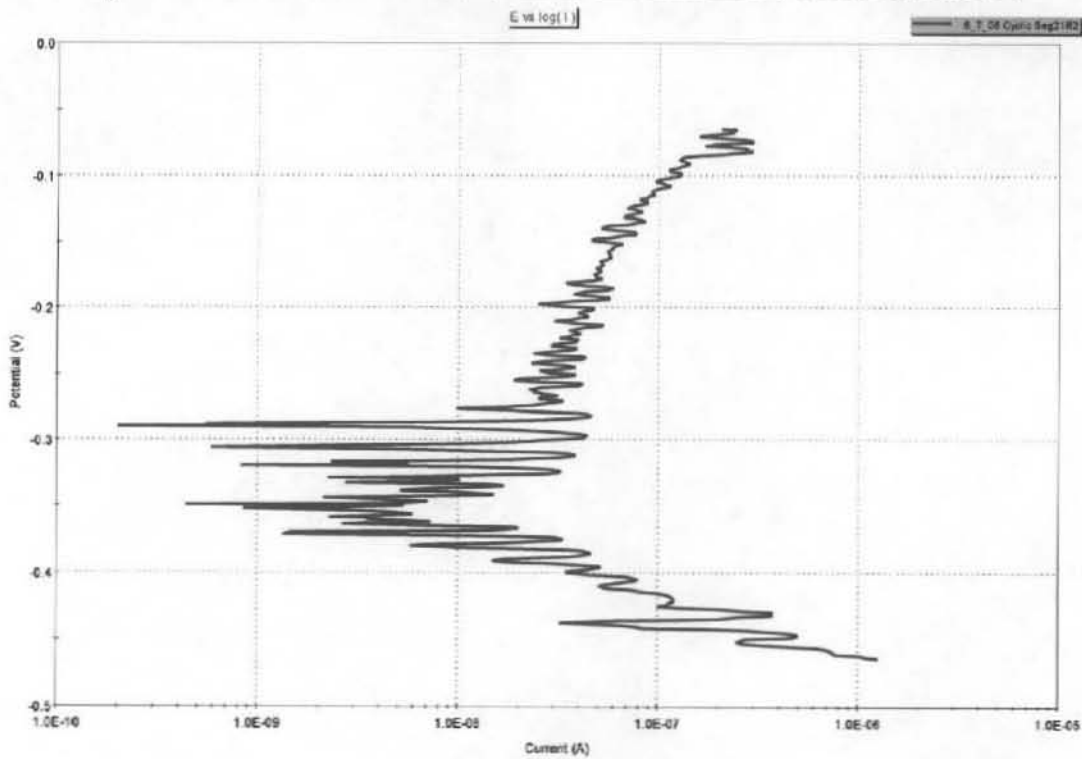**Figure B-9. Tank 241-AN-107, Anaerobic Extrusion, Interstitial Liquid vs. SCE.**

Figure B-10. Tank 241-AN-107, Anaerobic Extrusion, Saltcake vs. SCE.


B-5

RPP-RPT-34697, Rev. 0

APPENDIX C

General Relationship between Corrosion and Electrochemistry

RPP-RPT-34697, Rev. 0

Corrosion is a process involving electrochemical oxidation and reduction reactions. When a metal is immersed in a given solution, electrochemical reactions characteristic of the metal-solution interface occur at the surface of the metal causing the metal to corrode. These reactions create an electrochemical potential called the corrosion potential (E_{CORR}) or the open circuit potential (OCP) measured in volts at the metal-solution interface. The corrosion potential cannot be directly measured and must be determined by difference in potential with a known reference system. For iron in an acid solution, two reactions are occurring. The iron metal is being oxidized (reaction in which an atom loses electrons) and hydrogen ions are being reduced (reaction in which an atom gains electrons) (Princeton Applied Research, "Basics of Corrosion Measurements"):

$$Fe \rightarrow Fe^{+2} + 2e^-$$
$$2H^+ + 2e^- \rightarrow H_2$$
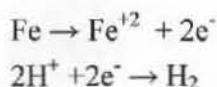
At E_{CORR}, the rate of oxidation is exactly equal to the rate of the reduction process, and the system is in equilibrium. If a potential is imposed on the metal specimen, other than E_{CORR}, the specimen is polarized. This polarization results in the oxidation or reduction reaction to become predominate at the metal surface, giving rise to a current (i). The current can be related to the rate of the electrochemical reactions. Potentials positive to E_{CORR} will accelerate the oxidation reaction creating an anodic current (i_{OX}) and is displayed with a positive polarity. Potentials negative to E_{CORR} will accelerate the reduction reaction and create a cathodic current (i_{RED}) displayed with a negative polarity. Only the total current (i_{Total}) can be measured at the metal specimen. At E_{CORR}, the $i_{Total} = i_{RED} + i_{OX} = 0$ because the currents flow in opposite directions. By polarizing the specimen in a systematic manner and measuring the resulting current, the value of i_{OX} or i_{RED} can be determined at E_{CORR}. These polarization measurements are the basis for electrochemical corrosion studies. By polarizing the specimen, it is also possible to accelerate passivation, pitting, or other slow corrosion processes.

Most laboratory electrochemical corrosion tests are performed in a test cell containing the solution to be tested. The specimen to be tested when immersed in the solution is called the working electrode. The reference electrode contacts the solution by a bridge tube, which consists of a ceramic frit interface, and the test solution or other electrolyte. Counter electrodes of graphite or platinum are used to supply the current flowing at the working electrode during the test. The cell is configured to allow purging with an inert gas to remove oxygen that may impact the corrosion reactions. A potentiostat is used to control the potential difference between the reference and working electrode and measure the current between the working electrode and the counter electrode.

In potentiodynamic measurements, the electrode potential is slowly scanned (0.1-10 mV/sec) and the resulting current is measured. Scans within ±25 mV of E_{CORR} may be used in polarization resistance measurements to measure R_P, which is the resistance of the specimen to oxidation during polarization. This value may then be used in calculations to determine corrosion rates and the corrosion current (i_{CORR}). Tafel plots are performed over ±250 mV of E_{CORR} and permit the estimation of Tafel constants that are used in the calculation of corrosion rates and current. Potentiodynamic scans over larger potential regions can identify passivation and transpassive areas of the corrosion system. Active-passive regions that can indicate potential for stress

C-1

RPP-RPT-34697, Rev. 0

corrosion cracking can also be identified from the scan. Cyclic polarization where the potential is reversed to the negative (cathodic) direction may be used to evaluate the pitting tendencies of materials. The configuration of the cell and control of the potentiostat are used to perform different electrochemical measurements to understand the corrosion behavior of materials under varying conditions.

C.1 POLARIZATION RESISTANCE

The electrochemical measurement of polarization resistance is used to determine absolute corrosion rates, expressed in mils per year (mpy). Polarization resistance measurements can be executed very rapidly. Excellent correlation may be made between corrosion rates obtained by polarization resistance and conventional weight-loss determinations. This technique is also referred to as "linear polarization."

As mentioned in Section 2, the polarization resistance measurement is performed by scanning through a potential range, which is very close to the corrosion potential (E_{CORR}), generally ± 25 mV versus E_{CORR}. The corrosion current i_{CORR}, is related to the response of the scanning potential versus current through the equation:

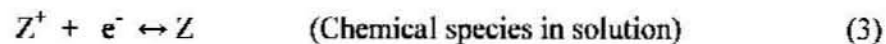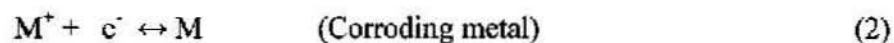$$\Delta E / \Delta i = (\beta_A \beta_C) / [2.3 (i_{CORR})(\beta_A + \beta_C)] \tag{1}$$

where

> $\Delta E / \Delta I$ = The slope of the polarization resistance plot. ΔE has units of volts and Δi has units of microamps (μA). The slope has units of resistance, hence, polarization resistance.

> β_A, β_C = Anodic and cathodic Tafel constants. These must be determined from a Tafel plot (see Section 2.2). The constants have units of volts/decade of current (may be expressed as mV/decade also).

> i_{CORR} = Corrosion current, μA.

A theoretical background for polarization resistance measurements emanated from the work of Stern and Geary 1957. Basically, in a corroding system, two coexisting electrochemical reactions are present:

$$M^+ + e^- \leftrightarrow M \qquad \text{(Corroding metal)} \tag{2}$$

$$Z^+ + e^- \leftrightarrow Z \qquad \text{(Chemical species in solution)} \tag{3}$$

The equilibrium potentials of the couples in Equation 2 and Equation 3 are labeled $E_{EQ,M}$ and $E_{EQ,Z}$, respectively. When the corrosion potential is sufficiently removed from $E_{EQ,M}$ and $E_{EQ,Z}$, the rate of reduction of M^+ becomes insignificant compared to the rate of oxidation of M and, likewise, the rate of oxidation of Z becomes insignificant with respect to the rate of reduction of Z^+. The corrosion potential, therefore, is the potential at which the rate of oxidation of M

C-2

RPP-RPT-34697, Rev. 0

(defined by current $i_{O,M}$) is equal to the rate of reduction of Z (defined by the current $i_{R,Z}$). Since the net current is the difference between the oxidation and reduction currents, the current measured (i_{MEAS}) with an external device will be zero.

$$i_{MEAS} = i_{O,M} - i_{R,Z} = 0 \text{ at } E_{CORR} \tag{4}$$

To calculate the corrosion rate, i_{CORR} must be determined.

When a potential is imposed on the metal specimen from an external voltage source, such as a potentiostat, a current will pass according to the following equation:

$$i_{MEAS} = i_{O,M} - i_{R,Z} \tag{5}$$

The anodic and cathodic currents obey the Tafel equation (see Section 2.2):

$$\eta = \beta_A \log (i_{O,M} / i_{CORR}) \tag{6}$$

$$\eta = - \beta_C \log (i_{R,Z} / i_{CORR}) \tag{7}$$

where

$\eta =$ The overvoltage, the difference between the potential imposed on the specimen and the corrosion potential, or $E_{APP} - E_{CORR}$.

Equations 6 and 7 are rearranged to yield

$$\log (i_{O,M} / i_{CORR}) = \eta / \beta_A \tag{8}$$

$$\log (i_{R,Z} / i_{CORR}) = - \eta / \beta_C \tag{9}$$

Taking the transform of Equations 8 and 9 yields

$$10^{\eta / \beta_A} = i_{O,M} / i_{CORR} \tag{10}$$

$$10^{-\eta / \beta_C} = i_{R,Z} / i_{CORR} \tag{11}$$

Now, substituting Equations 10 and 11 into Equation 4, yields

$$i_{MEAS} = i_{CORR} (10^{\eta / \beta_A} - 10^{-\eta / \beta_C}) \tag{12}$$

Since using a power series may approximate 10^x, and if x is a small value, then the third and later terms may be neglected without significant error. Therefore, substituting the term η / β_A for x, the power series collapses into

$$10^{\eta / \beta_A} = 1 + 2.3 \eta / \beta_A \tag{13}$$

C-3

RPP-RPT-34697, Rev. 0

$$10^{-\eta/\beta_C} = 1 - 2.3 \; \eta / \; \beta_C \qquad (14)$$

Substituting Equations 13 and 14 into Equation 12 and simplifying yields

$$i_{MEAS} = 2.3 \; i_{CORR} \; \eta \; (\beta_A + \beta_C \; / \; \beta_A \; \beta_C) \qquad (15)$$

Rearranging to solve for polarization resistance yields Equation 16, which is identical to Equation 1:

$$\eta / i_{MEAS} = \; \beta_A \; \beta_C \; / \; (2.3 \; i_{CORR} \; (\beta_A + \beta_C)) \qquad (16)$$

For the most accurate results, the Tafel constants, β_A and β_C, must be independently determined from a Tafel plot.

C.2   TAFEL PLOT

A Tafel plot is performed on a metal specimen by polarizing the specimen 250 mV cathodically and 250 mV anodically from the corrosion potential (E_{CORR}) and measuring the associated current. Figure 1 depicts a Tafel plot. The convergence of the cathodic (lower) and anodic (upper) polarization curves (i.e., the spike on the Figure 1 curve) represents E_{CORR}. The intersection of the lines tangent to the cathodic and anodic Tafel slopes are at i_{CORR} as shown in Figure 1.

Figure 1. Example of Tafel Plot.

C-4
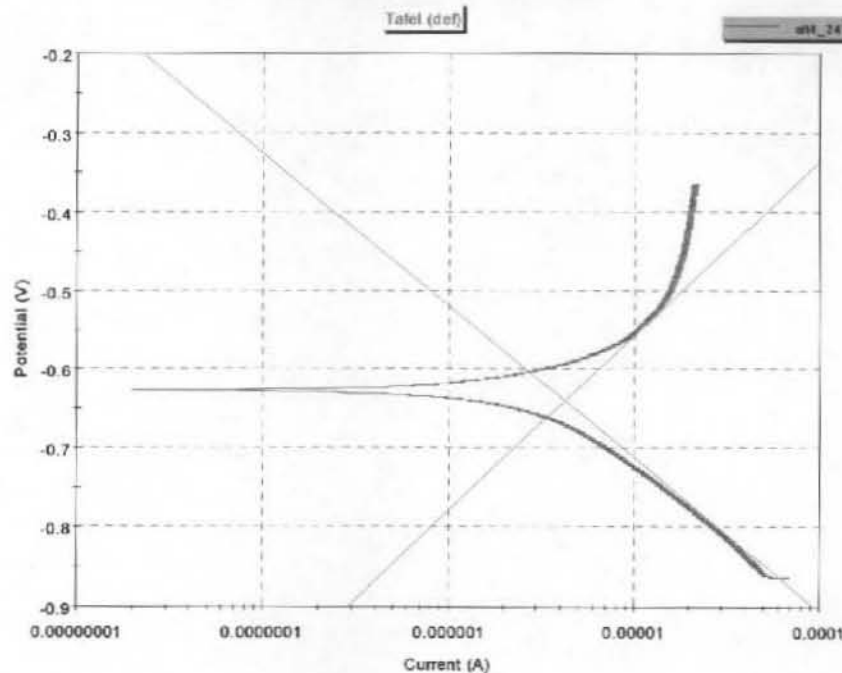
RPP-RPT-34697, Rev. 0

The anodic or cathodic Tafel plots are described by the Tafel equation.

$$\eta = \beta \log (i / i_{CORR}) \qquad (17)$$

where

η = The overvoltage, the difference between the potential of the specimen and the corrosion potential.

β = Tafel constant.

i_{CORR} = Corrosion current, μA.

i = Current at overvoltage η, μA.

Rearrangement of Equation 17 yields

$$\eta = \beta (\log i - \log i_{CORR}) \qquad (18)$$

Equation 18 is in the form of a straight line, $y = mx + b$. A plot of η versus log i is a straight line with slope β. Tafel constants must be calculated from the cathodic and anodic portions of the Tafel plot. The units of the Tafel constant are either in mV/decade of current or V/decade of current. A decade of current is one order of magnitude.

C.3 CORROSION RATE CALCULATION

According to Faraday's Law:

$$Q = (nFW) / M \qquad (19)$$

where

Q = Coulombs
n = The number of electrons involved in the electrochemical reaction.
F = The Faraday constant with a value of 96,487 coulombs.
W = The weight of the electroactive species.
M = The molecular weight of the electroactive species.

Rearranging Equation 19,

$$W = QM / nF,$$

and since equivalent weight $E_{wt} = M/n$, then

$$W = (QE_{wt}) / F$$

RPP-RPT-34697, Rev. 0

Since $Q = i * t$ from Faraday's Law,

$$W = (i * t * E_{wt}) / F \qquad (20)$$

where

    i = current
    t = time

The term W/t is the corrosion rate (C.R.) in grams/second. It is convenient and traditional to express corrosion rate as mpy. These units provide an indication of penetration.

Dividing Equation 20 by the electrode area (A) and the material's density (d) gives

$$\text{C.R. (cm/sec)} = (i * E_{wt} / d \, FA) \qquad (21)$$

Converting the seconds to years and centimeters to milli-inches, the Faraday (amp – sec/eq) to μA yields

$$\text{C.R. (mpy)} = (i * E_{wt} * 31.6 * 10^6 * 10^3) / (dFA * 2.5 * 10^6) \qquad (22)$$

Expressing the terms i/A as current density and combining all the constants yields

$$\text{C.R. (mpy)} = (0.13 * i_{CORR} * E_{wt}) / d \qquad (23)$$

where

    i_{CORR} = Corrosion current density, $\mu A / cm^2$.

    E_{wt} = Equivalent weight of the corroding species, in grams.

    d = Density of the corroding species, g/cm^3.

Equation 23 is used to calculate the corrosion rate directly from i_{CORR}, which is determined from the Tafel plot after a potentiodynamic scan.